

วิธีใหม่สำหรับการวิเคราะห์พัลส์ไฟต์/พัลส์เฟอริไดออกไซด์
โดยซีเควินเซียลอินเจกชันที่ใช้ขั้วไฟฟ้าเพชรที่โดปด้วยโบรอน



นาย ชากร ชินวงศ์อมร

สถาบันวิทยบริการ
จุฬาลงกรณ์มหาวิทยาลัย
วิทยานิพนธ์นี้เป็นส่วนหนึ่งของการศึกษาตามหลักสูตรปริญญาวิทยาศาสตรดุษฎีบัณฑิต

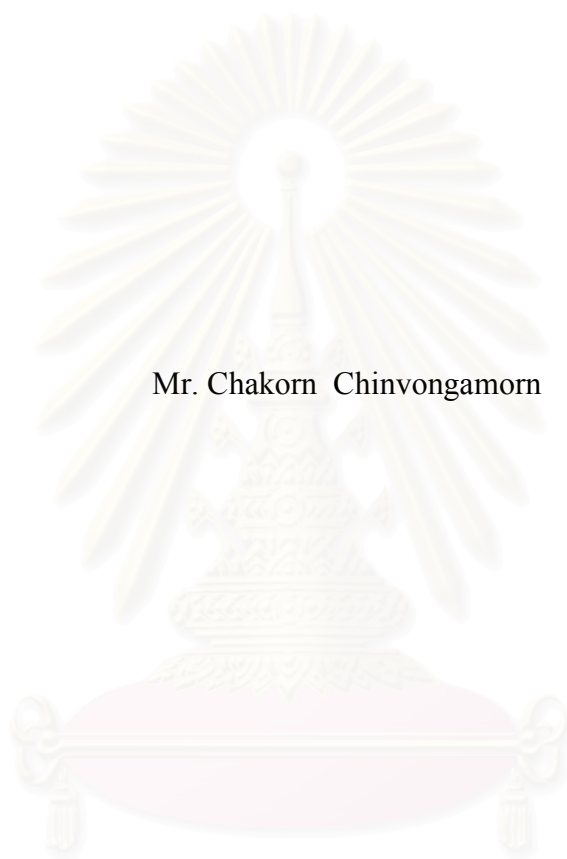
สาขาวิชาเคมี ภาควิชาเคมี

คณะวิทยาศาสตร์ จุฬาลงกรณ์มหาวิทยาลัย

ปีการศึกษา 2550

ลิขสิทธิ์ของจุฬาลงกรณ์มหาวิทยาลัย

NOVEL METHOD FOR ANALYSIS OF SULFITE/SULFUR DIOXIDE
USING SEQUENTIAL INJECTION WITH BORON-DOPED DIAMOND ELECTRODE



Mr. Chakorn Chinvongamorn

สถาบันวิทยบริการ
จุฬาลงกรณ์มหาวิทยาลัย
A Dissertation Submitted in Partial Fulfillment of the Requirements
for the Degree of Doctor of Philosophy Program in Chemistry

Department of Chemistry

Faculty of Science


Chulalongkorn University

Academic Year 2007

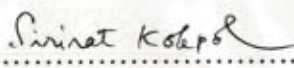
Copyright of Chulalongkorn University


Thesis Title NOVEL METHOD FOR ANALYSIS OF SULFITE/
SULFUR DIOXIDE USING SEQUENTIAL INJECTION
WITH BORON-DOPED DIAMOND ELECTRODE
By Mr. Chakorn Chinvongamorn
Field of Study Chemistry
Thesis Advisor Associate Professor Orawon Chailapakul, Ph.D.
Thesis Co-advisor Assistant Professor Narong Praphairaksit, Ph.D.


Accepted by the Faculty of Science, Chulalongkorn University in Partial
Fulfillment of the Requirements for the Doctoral Degree


..... Dean of the Faculty of Science
(Professor Supot Hannongbua, Ph.D.)

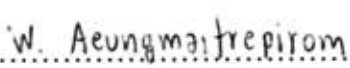
THESIS COMMITTEE

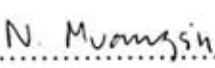

..... Chairman
(Associate Professor Sirirat Kokpol, Ph.D.)


..... Thesis Advisor
(Associate Professor Orawon Chailapakul, Ph.D.)


..... Thesis Co-advisor
(Assistant Professor Narong Praphairaksit, Ph.D.)


..... External Member
(Assistant Professor Duangjai Nacapricha, Ph.D.)


..... Member
(Assistant Professor Wanlapa Aeungmaitrepirom, Ph.D.)


..... Member
(Associate Professor Nongnuj Muangsin, Ph.D.)

ชาคร ชินวงศ์อมร : วิธีใหม่สำหรับการวิเคราะห์ซัลไฟต์/ซัลเฟอร์ไดออกไซด์โดยใช้เควิน
 เซียลอินเจกชันที่ใช้ขั้วไฟฟ้าเพชรที่โดปด้วยโบรอน (NOVEL METHOD FOR ANALYSIS
 OF SULFITE/SULFUR DIOXIDE USING SEQUENTIAL INJECTION WITH BORON-
 DOPED DIAMOND ELECTRODE) อ.ที่ปรึกษา: รศ. ดร. อรวรรณ ชัยลภากุล; อ.ที่ปรึกษา
 ร่วม: ผศ. ดร. ณรงค์ ประไพรัชสิทธิ์; 80 หน้า.

ได้พัฒนาระบบซีเควินเซียลอินเจกชันที่ใช้ร่วมกับหน่วยแยกแก๊สสำหรับการหาปริมาณ
 ซัลไฟต์/ซัลเฟอร์ไดออกไซด์โดยใช้เทคนิคแอมเพอโรเมทรีที่ใช้ขั้วไฟฟ้าเพชรที่โดปด้วยโบรอน
 สำหรับการตรวจวัด หน่วยแยกแก๊สทำหน้าที่ป้องกันสารรบกวนจากเมทริกในตัวอย่างซึ่งมีผลต่อ
 การตรวจวัดทางเคมีไฟฟ้า ในการวิเคราะห์ได้ผสมสารตัวอย่างกับสารละลายกรดเพื่อทำให้เกิด
 แก๊สซัลเฟอร์ไดออกไซด์แล้วผ่านสารละลายผสมไปยังหน่วยแยกแก๊ส แก๊สซัลเฟอร์ไดออกไซด์ที่
 เกิดขึ้นจะแพร่ผ่านเมมเบรนที่มีความจำเพาะต่อแก๊สเข้าไปยังสารละลายตัวพาซึ่งเป็นสารละลาย
 ผสมระหว่างสารละลายฟอสเฟตบัฟเฟอร์ (พีเอช 8) เข้มข้น 0.1 โมลาร์ กับสารละลายโซเดียม
 โดเดซิลซัลเฟตเข้มข้น 0.1 เปอร์เซ็นต์ และเปลี่ยนเป็นซัลไฟต์ ซัลไฟต์จะถูกพาไปยังเซลล์เคมี
 ไฟฟ้าเพื่อทำการตรวจวัดด้วยเทคนิคแอมเพอโรเมทรีที่ใช้ขั้วไฟฟ้าเพชรที่โดปด้วยโบรอนที่
 ศักย์ไฟฟ้า 0.95 โวลต์ (เทียบกับซิลเวอร์/ซิลเวอร์คลอไรด์) วิธีนี้ใช้ได้ในช่วงความเข้มข้นของ
 ซัลไฟต์ 0.2–20 มิลลิกรัมต่อลิตร เมื่อใช้สารตัวอย่าง 50 ไมโครลิตร และให้ค่าขีดจำกัดต่ำสุดของ
 การตรวจวัด 0.05 มิลลิกรัมต่อลิตร ได้นำวิธีนี้ไปประยุกต์หาปริมาณซัลเฟอร์ไดออกไซด์ในไวน์
 พบว่าได้ผลการวิเคราะห์สอดคล้องกับผลที่ได้จากวิธีไอโอดิเมทรีไทเทรชัน ค่าเบี่ยงเบนมาตรฐาน
 สัมพัทธ์ของปริมาณซัลเฟอร์ไดออกไซด์ที่ตรวจวัดได้ในไวน์อยู่ในช่วง 1.0–4.1 เปอร์เซ็นต์ อัตรา
 การตรวจวัดตัวอย่างคือ 65 ตัวอย่างต่อชั่วโมง

สถาบันนวัตกรรมการ
 จุฬาลงกรณ์มหาวิทยาลัย

ภาควิชา.....เคมี.....ลายมือชื่อนิสิต.....ชาคร ชินวงศ์อมร
 สาขาวิชา.....เคมี.....ลายมือชื่ออาจารย์ที่ปรึกษา.....อรวรรณ ชัยลภากุล
 ปีการศึกษา...2550.....ลายมือชื่ออาจารย์ที่ปรึกษาร่วม.....ณรงค์ ประไพรัชสิทธิ์

467 38056 23: MAJOR CHEMISTRY

KEY WORD: SULFITE / SULFUR DIOXIDE / SEQUENTIAL INJECTION ANALYSIS / BORON-DOPED DIAMOND ELECTRODE / GAS DIFFUSION UNIT

CHAKORN CHINVONGAMORN: NOVEL METHOD FOR ANALYSIS OF SULFITE/SULFUR DIOXIDE USING SEQUENTIAL INJECTION WITH BORON-DOPED DIAMOND ELECTRODE. THESIS ADVISOR: ASSOC. PROF. ORAWON CHAILAPAKUL, Ph.D., THESIS COADVISOR: ASSIST. PROF. NARONG PRAPHAIRAKSIT, Ph.D., 80 pp.

A gas diffusion sequential injection system with amperometric detection using a boron-doped diamond electrode was developed for the determination of sulfite/sulfur dioxide. A gas diffusion unit (GDU) was used to prevent interference from sample matrices for the electrochemical measurement. The sample was mixed with an acid solution to generate gaseous sulfur dioxide prior to its passage through the donor channel of the GDU. The sulfur dioxide diffused through the PTFE hydrophobic membrane into a carrier solution of 0.1 M phosphate buffer (pH 8)/0.1% sodium dodecyl sulfate in the acceptor channel of the GDU and turned to sulfite. Then the sulfite was carried to the electrochemical flow cell and detected directly by amperometry using the boron-doped diamond electrode at 0.95 V (versus Ag/AgCl). For sample volume of 50 μL , this method was applicable in the concentration range of 0.2 – 20 mg L^{-1} for sulfite and a detection limit (S/N = 3) of 0.05 mg L^{-1} for sulfite was achieved. This method was successfully applied to the determination of sulfur dioxide in wines and the analytical results agreed well with those obtained by iodimetric titration. The relative standard deviations for the analysis of sulfite in wines were in the range of 1.0 – 4.1 %. The sampling frequency was 65 h^{-1} .

Department.....Chemistry.....Student's signature.....*Chakorn Chinvongamorn*
 Field of study....Chemistry.....Advisor's signature.....*Orawon Chailapakul*
 Academic year...2007.....Co-advisor's signature.....*Narong Praphairaksit*

ACKNOWLEDGEMENTS

First of all, I would like to thank my thesis adviser, Associate Professor Dr. Orawon Chailapakul and my thesis co-advisor, Assistant Professor Dr. Narong Praphairaksit for their invaluable guidance, kind advices and encouragement. In addition, I would like to thank other members of the thesis committee for their extensive and excellent comments on early works and drafts of the thesis.

Furthermore, my great thanks go to the Thailand Research Fund through the Royal Golden Jubilee Ph.D. Program (Grant No. PHD/0247/2546) and the 90th Anniversary of Chulalongkorn University Fund (Ratchadphiseksomphot Endowment Fund) for the financial support.

Special thanks are also extended to Professor Dr. Toshihiko Imato (Kyushu University) for his kindness, valuable experience and provision of equipment during my stay in Japan. Moral supports and encouragement of my friends and all members of the electroanalytical chemistry research group of Chulalongkorn University are truly appreciated.

Finally, I would like to express my deepest gratitude and sincerest thank to my parents and family for their understanding and encouragement throughout the entire course of study.

สถาบันวิทยบริการ
จุฬาลงกรณ์มหาวิทยาลัย

CONTENTS

	PAGE
ABSTRACT (IN THAI)	iv
ABSTRACT (IN ENGLISH)	v
ACKNOWLEDGEMENTS	vi
CONTENTS	vii
LIST OF TABLES	x
LIST OF FIGURES	xii
ABBREVIATIONS	xv
CHAPTER I INTRODUCTION	1
1.1 Introduction.....	1
1.2 Research Objective.....	2
1.3 Scope of Research.....	2
CHAPTER II THEORY AND LITERATURE SURVEY	3
2.1 Fundamental of Electrochemistry.....	3
2.1.1 Cyclic Voltammetry.....	4
2.1.2 Hydrodynamic Voltammetry.....	6
2.1.3 Amperometric Detection.....	8
2.1.4 Boron-Doped Diamond Thin Film Electrode.....	9
2.2 Flow–Analysis Techniques.....	11
2.2.1 Flow Injection Analysis.....	11
2.2.2 Sequential Injection Analysis.....	12
2.3 Gas Diffusion Unit.....	14
2.4 Sulfites.....	19
2.4.1 Forms of Sulfite and Antimicrobial Activity.....	19
2.4.2 Sulfites Allergies.....	21
2.4.3 Amounts in Food and Regulations.....	21
2.4.4 Sulfur Dioxide in Wine.....	22
2.4.5 Methods for Sulfite/Sulfur dioxide Determination.....	23

	PAGE
CHAPTER III EXPERIMENTAL	26
3.1 Apparatus.....	26
3.2 Chemicals.....	27
3.3 Preparation of Solutions.....	28
3.3.1 Reagents Used in Cyclic Voltammetry.....	28
3.3.2 Reagents Used in Sequential Injection Analysis.....	28
3.3.3 Reagents Used in Iodimetric Titration.....	29
3.4 Cyclic Voltammetry.....	29
3.4.1 pH Dependence.....	30
3.4.2 Comparison of BDD Electrode with Glassy Carbon Electrode...	30
3.4.3 The Scan Rate Dependence Study.....	30
3.5 Sequential Injection with Amperometric Detection.....	30
3.5.1 Optimum Potential for Amperometric Detection.....	33
3.5.2 Effect of Sodium Dodecyl Sulfate.....	33
3.5.3 Sequential Injection Parameters.....	34
3.5.3.1 Sequence of Sulfite and Acid Aspiration.....	34
3.5.3.2 Volume of Sulfuric Acid.....	35
3.5.3.3 Propelling Flow Rate.....	35
3.5.3.4 Flow Rate of Carrier.....	36
3.5.4 Influence of Sample Volume.....	36
3.5.5 Linearity.....	36
3.5.6 Limit of Detection.....	36
3.5.7 Repeatability.....	37
3.6 Real Sample Analysis.....	37
3.6.1 Effect of Ethanol.....	37
3.6.2 Determination of Sulfur Dioxide in Wines by Developed SIA...	37
3.6.3 Determination of Sulfur Dioxide in Wines by Iodimetric Titration.....	38
CHAPTER IV RESULTS AND DISCUSSION	39
4.1 Cyclic Voltammetry Measurement.....	39
4.1.1 pH Dependence.....	39

	PAGE
4.1.2 Comparison of BDD Electrode with Glassy Carbon Electrode...	41
4.1.3 The Scan Rate Dependence Study.....	43
4.2 Sequential Injection with Amperometric Detection.....	44
4.2.1 Optimum Potential for Amperometric Detection.....	44
4.2.2 Effect of Sodium Dodecyl Sulfate.....	47
4.2.3 Sequential Injection Parameters.....	48
4.2.3.1 Sequence of Sulfite and Acid Aspiration.....	48
4.2.3.2 Volume of Sulfuric Acid.....	50
4.2.3.3 Propelling Flow Rate.....	55
4.2.3.4 Flow Rate of Carrier.....	57
4.2.4 Influence of Sample Volume.....	59
4.2.5 Linearity.....	60
4.2.6 Limit of Detection.....	62
4.2.7 Repeatability.....	63
4.3 Real Sample Analysis.....	64
4.3.1 Effect of Ethanol.....	64
4.3.2 Determination of Sulfur Dioxide in Wines.....	65
4.4 Comparison of the proposed SIA method with Other Methods	66
CHAPTER V CONCLUSIONS.....	68
5.1 Conclusions.....	68
5.2 Suggestion for Further Work.....	69
REFERENCES.....	70
APPENDICES.....	75
APPENDIX A Results for the determination of free and total SO ₂ in wines by SIA method	76
APPENDIX B Results for the determination of free and total SO ₂ in wines by titration method	78
VITA.....	80

LIST OF TABLES

TABLE	PAGE
2.1	Protocol sequence for the determination of sulfur dioxide in wines..... 16
2.2	Protocol sequence for determination of chlorine in waters..... 18
2.3	Protocol sequence for determination of chlorine in bleaches..... 18
2.4	Applications of sulfites in foods as antimicrobials and the concentration used..... 22
3.1	List of chemicals and their suppliers..... 27
3.2	The SIA operating sequence for sulfite analysis..... 33
3.3	The SIA operating sequence for sulfite analysis. The acid was aspirated after sulfite aspiration..... 34
3.4	The SIA operating sequence for analysis of sulfite. Another plug of acid was aspirated after sulfite aspiration..... 35
4.1	Comparison of electrochemical data obtained from cyclic voltammograms of 1 mM sodium sulfite at pH 4, 5, 6, 7, 8, 9, and 10..... 41
4.2	Electrochemical data for two SIA operating sequences: Sequence 1, sulfite aspiration after acid aspiration; Sequence 2, acid aspiration after sulfite aspiration..... 49
4.3	The average peak current and peak width for 10 mg L ⁻¹ sulfite at various volumes of 2 M H ₂ SO ₄ in the SIA operating sequence (step 2 in Table 3.2)..... 51
4.4	The average peak current and peak width for 50 mg L ⁻¹ sulfite at various volumes of 2 M H ₂ SO ₄ in the SIA operating sequence (step 2 in Table 3.2)..... 51
4.5	The average peak current and peak width for 10 mg L ⁻¹ sulfite at various volumes of 2 M H ₂ SO ₄ in the SIA operating sequence (step 4 in Table 3.4)..... 53
4.6	The average peak current and peak width for 50 mg L ⁻¹ sulfite at various volumes of 2 M H ₂ SO ₄ in the SIA operating sequence (step 4 in Table 3.4)..... 53
4.7	The average peak current and peak width for 10 mg L ⁻¹ sulfite at various flow rates for propelling the acidified sample to the GDU..... 57

TABLE	PAGE
4.8 The average peak current and peak width for 10 mg L ⁻¹ sulfite at various flow rates of carrier	59
4.9 The average peak current and peak width for 10 mg L ⁻¹ sulfite at various sample volumes.....	60
4.10 The average peak current and peak width for various concentrations of sulfite.....	61
4.11 Comparison of the results obtained by SIA and titration methods for free and total SO ₂ in wines.....	65
4.12 Comparison of analytical characteristics of the proposed SIA and some flow-based methods.....	67
A1 Linear equations of calibration curve for the calculation of free and total SO ₂ and dilution factor for the calculation of total SO ₂	76
A2 Signal currents obtained by SIA method and concentration of free and total SO ₂ in wine.....	77
B1 Concentration of standard I ₂ and volume of blank for the calculation of free and total SO ₂ in wines.....	78
B2 Volume of I ₂ obtained by titration method and concentration of free and total SO ₂ in wine.....	79

LIST OF FIGURES

FIGURE	PAGE
2.1	4
2.2	5
2.3	7
2.4	8
2.5	11
2.6	12
2.7	12
2.8	14
2.9	15
2.10	16
2.11	17
2.12	20
2.13	23
3.1	29
3.2	31
3.3	31
3.4	32
4.1	40

FIGURE	PAGE
4.2 Cyclic voltammograms of 1 mM Na ₂ SO ₃ in 0.1 M phosphate buffer solution (pH 8) at the BDD electrode (solid line) and the GC electrode (dash line). The scan rate was 50 mV s ⁻¹ . The area of electrode was 0.07 cm ²	42
4.3 Cyclic voltammograms of 0.1 M phosphate buffer solution (pH 8) as the background at the BDD electrode (solid line) and the GC electrode (dash line). The scan rate was 50 mV s ⁻¹ . The area of electrode was 0.07 cm ²	42
4.4 Cyclic voltammograms of 1 mM Na ₂ SO ₃ in 0.1 M phosphate buffer solution (pH 8) at various scan rates for the BDD electrode. The area of electrode was 0.07 cm ²	43
4.5 The relationship between the peak current and the square root of the scan rate (v ^{1/2}).....	44
4.6 Hydrodynamic voltammograms for 0.1 M phosphate buffer (pH 8)/0.1 % SDS (Background) at 0.70–1.05 V (vs. Ag/AgCl). The flow rate of carrier was 0.5 mL min ⁻¹	45
4.7 Hydrodynamic voltammogram for 10 mg L ⁻¹ SO ₃ ²⁻ (Signal) at 0.70–1.05 V (vs. Ag/AgCl). The SIA operating sequence was listed in Table 3.2. The flow rate of carrier was 0.5 mL min ⁻¹	45
4.8 Hydrodynamic voltammetric <i>i</i> -E curve for 10 mg L ⁻¹ SO ₃ ²⁻ (Signal) and 0.1 M phosphate buffer (pH 8)/0.1% SDS (Background).....	46
4.9 Relationship between potential and signal-to-background ratio.....	46
4.10 SIA with amperometric detection results for 15 consecutive injections of 10 mg L ⁻¹ SO ₃ ²⁻ . Carrier was 0.1 M phosphate buffer pH 8 (-□-) and 0.1 M phosphate buffer pH 8/0.1% SDS (-●-). The SIA operating sequence was listed in Table 3.2.....	47
4.11 SIA with amperometric detection results of 10 mg L ⁻¹ SO ₃ ²⁻ for two SIA operating sequences: Sequence 1, sulfite aspiration after acid aspiration; Sequence 2, acid aspiration after sulfite aspiration.....	48
4.12 SIA with amperometric detection results of 50 mg L ⁻¹ SO ₃ ²⁻ for two SIA operating sequences: Sequence 1, sulfite aspiration after acid aspiration; Sequence 2, acid aspiration after sulfite aspiration.....	49

FIGURE	PAGE
4.13 The relationship between the average peak current for 10 mg L ⁻¹ sulfite and the volume of 2 M H ₂ SO ₄ in the SIA operating sequence (step 2 in Table 3.2).....	52
4.14 The relationship between the average peak current for 50 mg L ⁻¹ sulfite and the volume of 2 M H ₂ SO ₄ in the SIA operating sequence (step 2 in Table 3.2).....	52
4.15 The relationship between the average peak current for 10 mg L ⁻¹ sulfite and the volume of 2 M H ₂ SO ₄ in the SIA operating sequence (step 4 in Table 3.4).....	54
4.16 The relationship between the average peak current for 50 mg L ⁻¹ sulfite and the volume of 2 M H ₂ SO ₄ in the SIA operating sequence (step 4 in Table 3.4).....	54
4.17 SIA with amperometric detection results for 10 mg L ⁻¹ sulfite at various flow rates for propelling the acidified sample to the GDU.....	56
4.18 SIA with amperometric detection results for 10 mg L ⁻¹ sulfite at various flow rates of carrier.....	58
4.19 The relationship between the average peak current and the sample volume for 10 mg L ⁻¹ sulfite.....	60
4.20 Calibration curve of sulfite.....	61
4.21 SIA with amperometric detection results for blank and 0.05 mg L ⁻¹ sulfite.....	62
4.22 SIA with amperometric detection results for ten consecutive injections of 10 mg L ⁻¹ sulfite.....	63
4.23 The relationship between the average peak current for 10 mg L ⁻¹ sulfite and the percent of ethanol in sulfite solution.....	64

ABBREVIATIONS

BDD	boron-doped diamond
CV	cyclic voltammetry
CVD	chemical vapor deposition
°C	degree Celsius
E	potential
E_p	peak potential
E_{pa}	anodic peak potential
E_{pc}	cathodic peak potential
EDTA	ethylenediaminetetraacetic acid
FI	flow injection
FIA	flow injection analysis
g	gram
GC	glassy carbon
GD	gas diffusion
GDU	gas diffusion unit
GD-FIA	gas diffusion-flow injection analysis
GD-SIA	gas diffusion-sequential injection analysis
h	hour
i	current
i_{pa}	anodic peak current
i_{pc}	cathodic peak current
L	liter
M	molar
min	minute
mL	milliliter
nA	nanoampere
R^2	correlation coefficient
s	second
SDS	sodium dodecyl sulfate
SI	sequential injection
SIA	sequential injection analysis

S/B	signal to background ratio
t	time
V	volt
v/v	volume by volume
w/v	weight by volume
μA	microampere
μL	microliter



สถาบันวิทยบริการ
จุฬาลงกรณ์มหาวิทยาลัย

CHAPTER I

INTRODUCTION

1.1 Introduction

Sulfites, or sulfiting agents, are widely used as additives in food and brewing industries to inhibit bacterial growth, prevent oxidation, and improve the final appearance of products. Despite these useful properties, the sulfite content in foods and beverages has been strictly limited due to its allergenic effect on hypersensitive people. Products containing more sulfite than the established threshold level must be adequately labeled. For example, in the United States, the Food and Drug Administration (FDA) has required labeling of products containing more than 10 mg L⁻¹ of sulfite in foods and beverages. Therefore, the method for sulfite analysis is of great importance for food assurance and quality control as well as beverages and pharmaceutical products.

Conventional methods for the analysis of sulfite, such as titration with iodine and acid/base titration after oxidation, usually need extensive sample pretreatment and reagent preparation. Flow injection analysis (FIA) and sequential injection analysis (SIA) which can be automated and used for a broad range of samples with high sampling frequency have also been applied to determine sulfite and sulfur dioxide. To improve selectivity, a gas diffusion unit (GDU) has been incorporated in flow systems to separate the liberated sulfur dioxide from sample matrices. Spectrometric and electrochemical detection are often coupled to flow systems for sulfite/sulfur dioxide determination. Spectrophotometric, fluorimetric, and chemiluminescence detection can be performed after mixing with some reagents, which results in cost and complication of the analysis as well as the toxicity of certain reagents. Electrochemical detection is an attractive option due to the direct electrochemical oxidation of sulfite.

A boron-doped diamond (BDD) electrode is an electrode material which offers a number of attractive electrochemical properties, including a wide potential window, low background current, and high electrochemical stability. The BDD electrode has been widely applied for the electrochemical detection of many types of analyte, such as biological compounds, organic pollutants, and metal ions.

Sequential injection analysis has been proposed as an alternative to flow injection analysis due to various advantages, such as lower reagent consumption and simple manifold, compared to FIA.

1.2 Research Objective

The gas diffusion sequential injection system with amperometric detection using the boron-doped diamond electrode is developed for the determination of sulfite/sulfur dioxide content. The developed method is then applied to the determination of sulfite/sulfur dioxide in real samples.

1.3 Scope of Research

The electrochemical properties of sulfite at boron-doped diamond electrode are investigated using cyclic voltammetry. Subsequently, the boron-doped diamond electrode is used for amperometric detection in the gas diffusion sequential injection system to find optimum conditions for sulfite detection. Finally, the gas diffusion sequential injection system with amperometric detection using the boron-doped diamond electrode is applied to the determination of sulfite/sulfur dioxide in real samples.



สถาบันวิทยบริการ
จุฬาลงกรณ์มหาวิทยาลัย

CHAPTER II

THEORY AND LITERATURE SURVEY

The fundamental of electrochemistry and electrochemical techniques used in this work are described in the initial section of this chapter. Consideration is then given to flow-analysis techniques and a gas diffusion unit coupled with flow system respectively. Finally the detail of sulfite is described.

2.1 Fundamental of Electrochemistry

Electrochemistry encompasses chemical and physical processes that involve the transfer of charge. There are two categories of electrochemical processes, potentiometric and electrolytic methods, that are applied to quantitative measurements. Potentiometry is the field of electroanalytical chemistry in which potential is measured under the conditions of no current flow. The measured potential may then be used to determine the analytical quantity of interest, generally the concentration of some component of the analyte solution. Unlike potentiometry, where the free energy contained within the system generates the analytical signal, electrolytic methods are an area of electroanalytical chemistry in which an external source of energy is supplied to drive an electrochemical reaction which would not normally occur. The externally applied driving force is either an applied potential or current. When potential is applied, the resultant current is the analytical signal; and when current is applied, the resultant potential is the analytical signal. Techniques which utilize applied potential are typically referred to as voltammetric methods while those with applied current are referred to as galvanostatic methods. Unlike potentiometric measurements, which employ only two electrodes, voltammetric measurements utilize a three electrode electrochemical cell. The use of three electrodes (working, auxiliary, and reference) along with the potentiostat instrument allows accurate application of potential functions and the measurement of the resultant current. The different voltammetric techniques are distinguished from each other primarily by the potential function that is applied to the working electrode to drive the reaction, and by the material used as the working electrode. In this section some voltammetric techniques used in this work such as cyclic voltammetry, hydrodynamic voltammetry, and

amperometric detection are considered respectively. Then the boron-doped diamond working electrode used in this work is described.

2.1.1 Cyclic Voltammetry [1-3]

Cyclic voltammetry (CV) is a very useful electroanalytical technique in many areas of chemistry. It is rarely used for quantitative determinations, but it is widely used for studying the mechanisms and reversibility of electrode processes. This technique is based on varying the applied potential at a working electrode in both forward and reverse directions while monitoring the current. For example, the initial scan could be in the negative direction to the switching potential. At that point the scan would be reversed and run in the positive direction. Depending on the analysis, one full cycle, a partial cycle, or a series of cycles can be performed. Some potential waveforms used in cyclic voltammetry are illustrated in Figure 2.1.

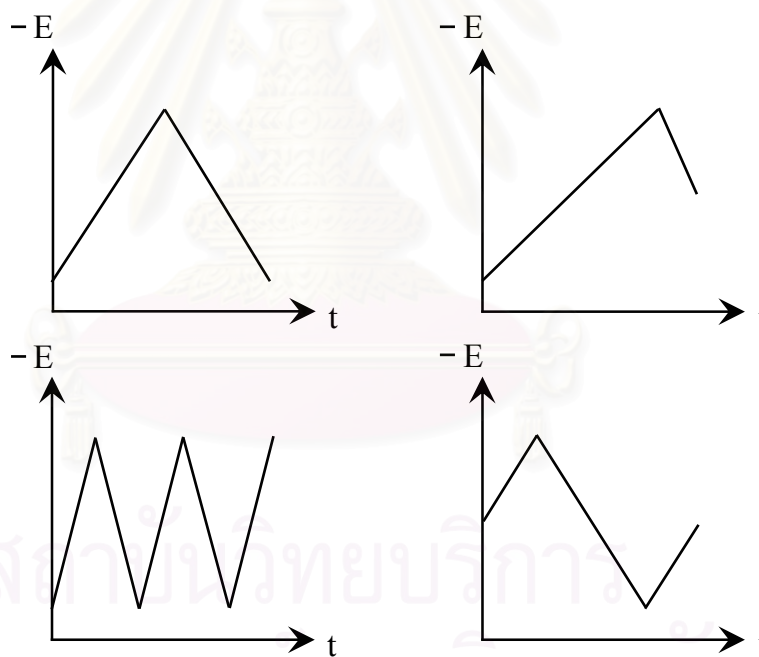


Figure 2.1 Some potential waveforms used in cyclic voltammetry.

The resulting plot of current versus potential is termed a cyclic voltammogram. The cyclic voltammogram can be very simple as shown in Figure 2.2 for the reversible, quasi-reversible and irreversible electrode processes. The voltammogram is characterized by a peak potential (E_p), at which the current reaches a maximum value and by the value of the peak current (i_p).

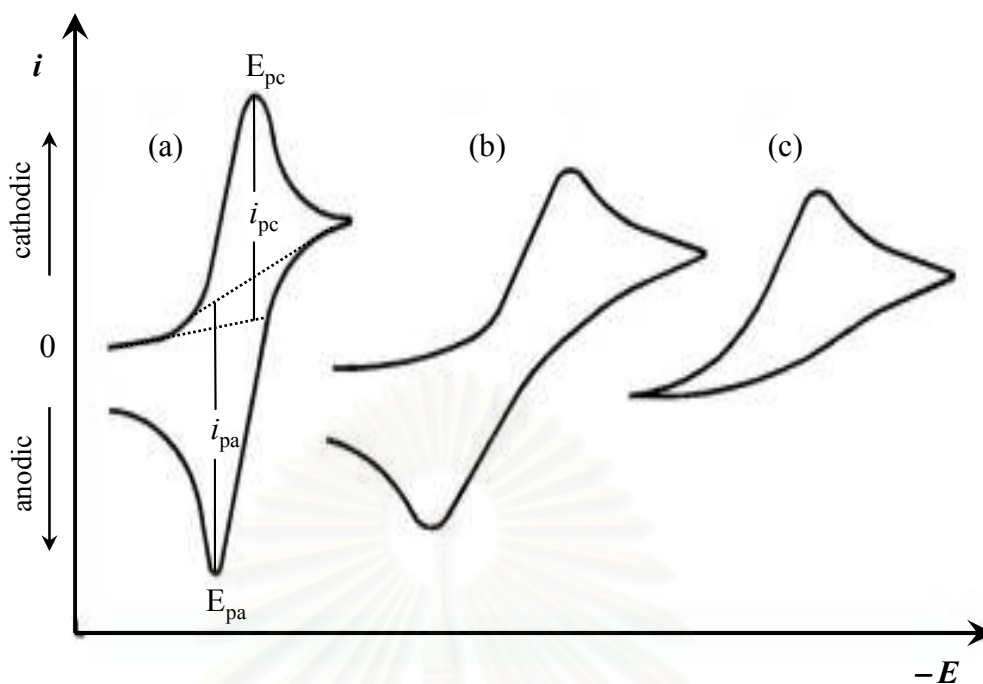


Figure 2.2 Cyclic voltammogram for a reversible (a), a quasi-reversible (b) and an irreversible (c).

If the electron transfer process is fast compared with other processes (such as diffusion), the reaction is said to be electrochemically reversible. The current-voltage cycle illustrated in Figure 2.2(a) for the reversible electrode process is obtained when the reaction products, formed during the forward scan as a result of the electrode reaction that gives rise to the peak at E_{pc} , are oxidized on the reverse scan as shown by the peak at E_{pa} . The peak current for a reversible couple (at 25°C) is given by the Randles-Sevcik equation:

$$i_p = 2.686 \times 10^5 n^{3/2} A c D^{1/2} \nu^{1/2}$$

where i_p is the peak current (amps), n is the number of electrons, A is the electrode area (cm^2), c is the concentration (mol cm^{-3}), D is the diffusion coefficient ($\text{cm}^2 \text{s}^{-1}$), and ν is the potential scan rate (V s^{-1}).

The separation between the peak potentials is given by

$$\Delta E_p = |E_{pa} - E_{pc}| = 2.303 RT / nF$$

Thus, for a reversible reaction at 25 °C with n electrons, ΔE_p should be $0.0592/n$ V or about 60 mV for one electron. In practice this value is difficult to attain

because of such factors as cell resistance. Irreversibility due to a slow electron transfer rate results in $\Delta E_p > 0.0592/n$ V.

For quasi-reversible systems shown in Figure 2.2(b), that are those which appear reversible in direct current polarography but give an irreversible response when faster measuring techniques are used, the difference in the peak potentials is about $60/n$ mV at low scan rates of 10 to 20 mV s^{-1} , but becomes greater as the scan rate is increased. Also, ΔE_p increases as the irreversibility of the electrode process increases.

For a totally irreversible process shown in Figure 2.2(c), that is one in which the electrode reaction products cannot be oxidized back to the initial analyte because k_{ox} is extremely small or because they have undergone a subsequent irreversible chemical change to compounds that are not electroactive, no anodic current peak is observed. Because of the dynamic nature of voltage-sweep voltammetry, irreversible processes give an expression for the peak current distinctly different from those of reversible systems:

$$i_p = 2.99 \times 10^5 n (\alpha n_a)^{1/2} A c D^{1/2} \nu^{1/2} \quad \text{at } 25^\circ\text{C}$$

where n_a represents the number of electrons in the rate-controlling step and α is the transfer coefficient (normally with a value between 0.3 and 0.7). The latter two quantities can be evaluated by taking the difference between the peak potential and the half-peak potential:

$$E_p - E_{p/2} = -0.048 / (\alpha n_a) \quad \text{at } 25^\circ\text{C}$$

An alternative approach is to scan the voltammogram at two different rates. Under these conditions α and n_a may be evaluated by the expression

$$(E_p)_2 - (E_p)_1 = \frac{RT}{\alpha n_a F} \ln \sqrt{\frac{\nu_1}{\nu_2}} \quad \text{at } 25^\circ\text{C}$$

2.1.2 Hydrodynamic Voltammetry [4]

In the hydrodynamic voltammetry the potential is applied while the solution is in motion toward the electrode. Hydrodynamic voltammetry is performed in several ways. One method involves stirring the solution vigorously while it is in contact with a fixed electrode. This method has low reproducibility and is practically

not used. Alternatively, the electrode is rotated at a constant high speed in the solution, thus providing the stirring action. Still another way of carrying out hydrodynamic voltammetry is to allow the analyte solution to flow through a tube in which the working electrode is mounted. This last technique is becoming widely used for detection and determination of oxidizable or reducible compounds or ions that have been separated by high-performance liquid chromatography or by flow injection methods. In these applications a thin layer cell such as that shown in Figure 2.3 is used. In these cells a three-electrode configuration is used. The auxiliary and reference electrodes are used along with the working electrode. The working electrode is typically imbedded in an insulating block. The voltage applied between the working electrode and the auxiliary electrode is always accompanied by an uncontrolled error due to the ohmic (IR) drop. In order to minimize this effect, the electrodes should be placed as close together as possible. The cell volume should be less than 5 μL in order to avoid any sensitivity loss or peak broadening caused by an unnecessarily large dead volume in the cell.

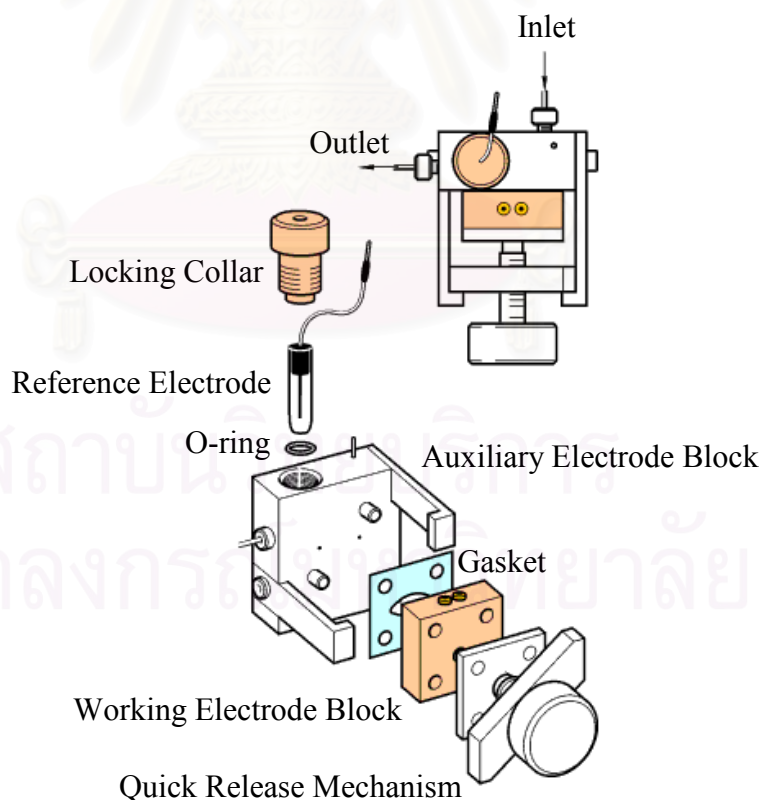


Figure 2.3 A thin layer cell from Bioanalytical Systems, Inc.

2.1.3 Amperometric Detection [5,6]

Amperometric detection has been developed as a sensitive method for chromatographic detection of electroactive solutes or as a detection method in conjunction with a selective biocatalytic step in biosensors. It has also been used as a detection method in flow-analysis techniques. Amperometric detection is based on oxidation or reduction of an electrochemically active analyte at a working electrode held at a potential that is high enough to initiate the oxidation or reduction process. The electric current resulting from this electrochemical reaction serves as the analytical signal and is directly proportional to the concentration of analyte. Generally, the flow conditions in measurements with amperometric detection decrease the thickness of the diffusion boundary layer at the working electrode surface. This results in an increase in the measured current.

The potential applied to the working electrode may be constant or it may be applied in a pulsed mode. Typical potential waveforms used in amperometric detection are illustrated in Figure 2.4.

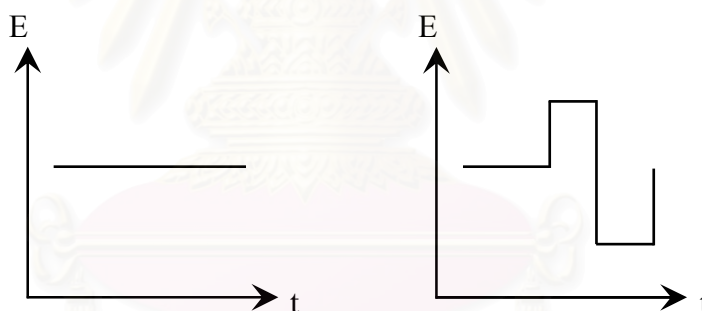


Figure 2.4 Typical potential waveforms used in amperometric detection.

Constant-potential amperometric detection at carbon, platinum or silver electrodes has been used in ion chromatography as a detection technique complementary to conductometric and photometric detection since the early developments of this separation technique. Applications (usually in the oxidative mode) include the determination of various ions like sulfite, nitrite, bromide, iodide, thiosulfate, thiocyanate, cyanide or arsenite. Triple-pulse and related waveforms are often used when the electrode surface is deactivated by products of the electrochemical reaction. In this case, the successive application of a measuring potential, a cleaning potential and a conditioning potential in a repetitive way (typical frequency of 1 to 2 Hz) can lead to a stable response. This is a well-known technique

in carbohydrate analysis but can also show significant advantages for inorganic ions such as sulfide. For metal ion detection, a bipolar waveform may be of advantage. Metal ions are reduced to the metallic state at the first potential and oxidized at the second potential, which is the measuring potential.

2.1.4 Boron-Doped Diamond Thin Film Electrode [7-9]

(a) Properties of Diamond

Diamond possesses several technologically important properties including extreme hardness, high electrical resistance, chemical inertness, high thermal conductivity, high electron and hole mobilities, and optical transparency. The material offers advantages for electronic applications under extreme environmental conditions.

(b) Synthesis of Conducting Diamond Materials

Undoped diamond is normally electrically insulating and cannot be used as an electrode material because of its large band gap of more than 5 eV. But diamond can be made conducting by doping it with certain elements. Currently, in most cases boron is used as dopant and the p-semiconductor results. If phosphorus or nitrogen is used as dopant the n-semiconductor is produced. Two major methods for the production of doped diamond materials have been developed: chemical vapor deposition (CVD) of thin film doped-diamond and high pressure, high temperature (HPHT) doped-diamond particle production. Other methods reported for the production of conducting diamond electrodes are vacuum annealing of undoped diamond and so-called surface transfer doping of undoped diamond.

For thin film CVD doped diamond, the doped diamond film is deposited on a conducting substrates which are usually either silicon or self-passivating metals such as titanium, tantalum, tungsten, molybdenum and niobium. The deposition technique is plasma-assisted CVD. The plasma necessary for the deposition is activated either by hot filaments or by microwave radiation. In both cases the gas phase typically consists of hydrogen as the carrier gas, methane or acetone/methane mixture as carbon source and other gases which provide dopants. By use of either microwave or thermally by hot filaments the gas phase is activated to

form the plasma. The carbon-containing gas is energetically activated to decompose the molecules into methyl radicals and atomic hydrogen if a methane hydrogen source gas mixture is used. Typical growth conditions are C/H volume ratios of 0.5-2%, pressures of 10-100 torr, substrate temperatures of 800-1000 °C, and microwave powers of 1000-1300 W, or filament temperatures of ~2100 °C, depending on the method used. The film grows by nucleation at rates in the 0.1-1 $\mu\text{m h}^{-1}$ range. For the substrates to be continuously coated with diamond, the nominal film thickness must be ~1 μm .

(c) Dopants for Diamond Electrodes

Boron is by far the most widely used dopant to produce conducting diamond electrodes. This is because boron has low charge carrier activation energy of 0.37 eV. Boron doping leads to a p-type semiconductor. At low doping levels, the diamond acts as an extrinsic semiconductor. At high doping levels the material acts as a semimetal. To introduce boron into the diamond material during film growth the boron containing substance has to be added to the deposition gas mixture. Substances such as diborane or trimethyl borane can be used. The boron atoms substitute in place of some of the carbon atoms during film growth. Boron-doped diamond electrodes with resistivities between 5 and 100 $\text{m}\Omega\text{-cm}$ are usually produced. Typical and useful boron concentrations in diamond are between 500 ppm to about 10,000 ppm or $10^{19} - 10^{21} \text{ atoms cm}^{-3}$.

Other dopants are also possible. They are introduced into the CVD diamond films by adding an appropriate gas to the deposition atmosphere. This is ammonia or N_2 in case of nitrogen doping, PH_3 for phosphorus and H_2S for sulfur doping.

(d) Electrochemical properties in aqueous electrolytes

Several interesting and important electrochemical properties distinguish boron-doped diamond thin films from conventional carbon electrodes. The films exhibit voltammetric background currents and double-layer capacitances up to an order of magnitude lower than that of glassy carbon. The low and stable background current and capacitance are attractive features of diamond for potentially improved signal-to-background ratio (S/B) in electrochemical assays. Another

interesting electrochemical property is that the films exhibit a wide working potential window for solvent-electrolyte electrolysis in conventional aqueous media, which means that a large overpotential exists for the evolution of chlorine, oxygen, and hydrogen. The larger overpotentials for diamond could possibly allow redox analytes with more positive and negative standard reduction potentials to be studied. Figure 2.5 is a comparison of the cyclic voltammetric current versus potential curves for boron-doped diamond thin film, glassy carbon and Hg electrodes in 0.1 M H₂SO₄.

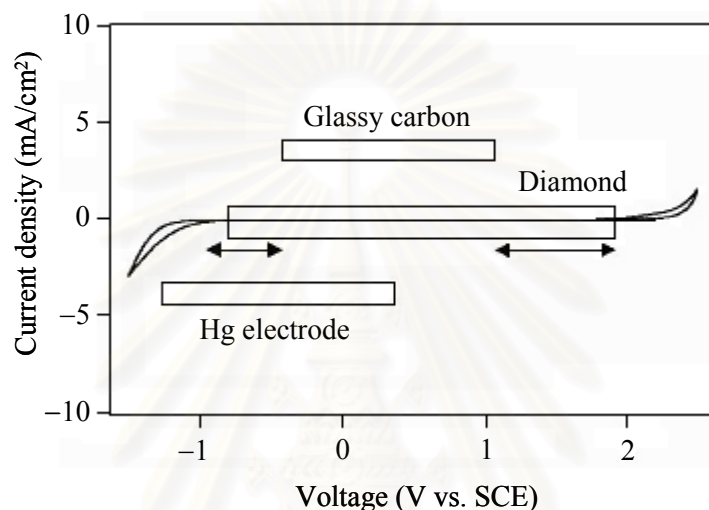


Figure 2.5 Cyclic voltammogram for diamond in 0.1 M H₂SO₄. The range of potential windows for glassy carbon and Hg electrodes are shown for comparison.

2.2 Flow–Analysis Techniques

Flow-based methods are well established and widely used as automated methods for analysis. In this section two flow-based methods, flow injection analysis and sequential injection analysis, are described.

2.2.1 Flow Injection Analysis [10]

Flow injection analysis (FIA) is a well-established continuous-flow technique that has proven its utility in both basic research and applications. This technique was initiated almost simultaneously by Ruzicka and Hansen [11] in Denmark and Stewart and coworkers [12] in the United States in the mid 1970s. The principle of this technique is to exploit controlled dispersion in narrow bore tubing, sometimes under the name of “zone fluidics”. A typical FIA manifold is illustrated in Figure 2.6. A volume of sample is inserted into the sample loop of an injection valve

while a stream of carrier and a stream of reagent are mixed at a confluence point and are flowing constantly through the detector. After the sample loop is filled with the sample, the valve is rotated so that the sample is injected into the flowing carrier stream and physically transported by the carrier to the confluence point where it mixes with the reagent. In the course of its travel through the reaction coil, the sample zone disperses and reacts with the reagent to form a detectable species. The detectable species gives rise to a transient peak when it passes through the flow-cell of the detector.

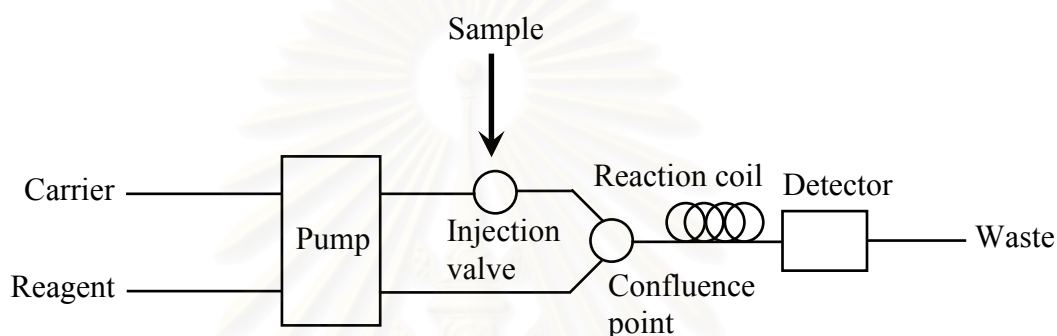


Figure 2.6 A typical manifold of flow injection analysis.

2.2.2 Sequential Injection Analysis [10,13,14]

Sequential injection analysis (SIA) was first proposed by Ruzicka and Marshall [15] in 1990 as a possible alternative to FIA. The principles upon which SIA is based are similar to those of FIA, namely controlled partial dispersion and reproducible sample handling. In contrast to FIA, SIA employs the computer-controlled multi-position selection valve and bi-directional pump operated synchronously.

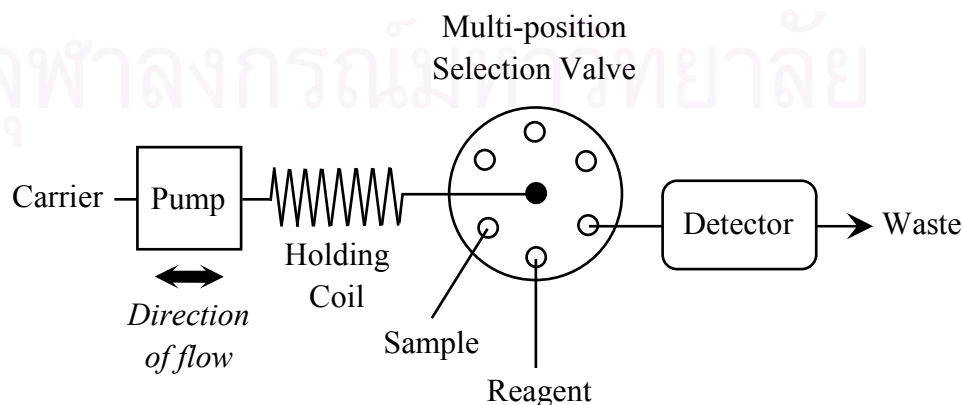


Figure 2.7 A typical manifold of sequential injection analysis.

A typical SIA manifold is illustrated in Figure 2.7. Propulsion of solution through the manifold tubing (typically 0.5–0.8 mm i.d. PTFE) is achieved using a peristaltic pump or a syringe pump. A holding coil is placed between the pump and the common port of the multi-position selection valve. The selection ports of the valve are coupled to sample and reagent reservoirs as well as a detector. The valve is directed to a selection port that is connected to the sample line and a zone of the sample is drawn up into the holding coil by the pump. Then, the selection valve is directed to a port that is connected to a reagent line and a zone of the reagent is drawn up into the holding coil adjacent to the sample zone. Then, the selection valve is switched to a port that is connected to a detector. As the zones move towards the detector, zone dispersion and overlap occurs, resulting in the formation of a detectable species that is monitored by the detector. The vast majority of SIA procedures are still based on the solution-phase chemistry described above.

Comparing SIA and FIA for this simple sample manipulation, the following points can be made:

- SIA makes use of a simpler, more robust single channel manifold even with multi-component chemical systems. In FIA, additional flow channels are required for each reagent.
- In SIA, the multi-channel peristaltic pumps commonly used in FIA are replaced by more accurate, robust syringe pumps.
- With SIA, the sample and reagent consumptions are drastically reduced.
- In SIA, the selection valve provides a means for performing convenient automated calibration.
- In SIA, accurate handling of sample and reagent zones necessitates computer control, so automation becomes essential.

In recent years, it has become apparent that the scope of SIA can be extended to encompass a variety of more complex, on-line, sample-manipulation and pretreatment procedures. Then, the ports of the multi-position selection valve are coupled to various units (e.g., reservoirs, detectors, pumps, reactors, separators, special cells, and other manifolds), as illustrated in Figure 2.8 [16]. After aspiration of the sample zone into the holding coil via the sample line, the sample can be

manipulated in different ways within the SIA manifold by taking advantage of the stopped-flow, bi-directional nature of fluid handling in SIA.

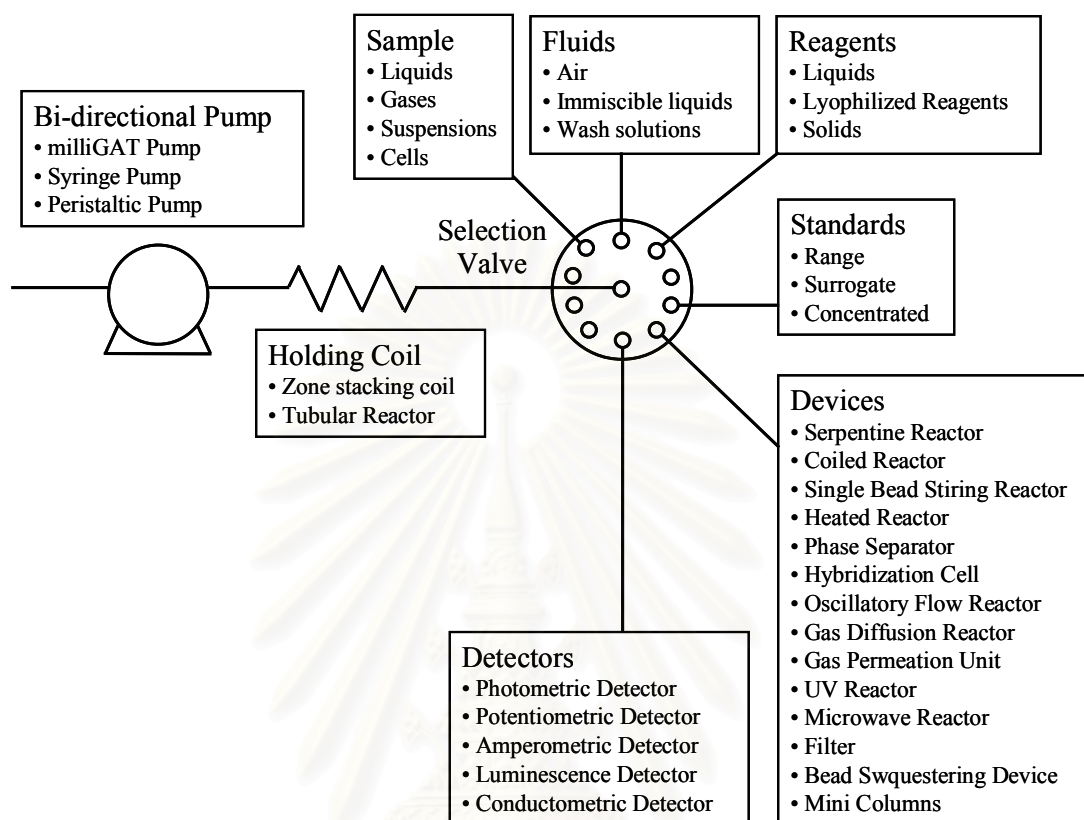


Figure 2.8 Potential of SIA for automated sample pre-treatment.

2.3 Gas Diffusion Unit [10,17]

Gas diffusion is commonly used in flow techniques to achieve both separation of the required analyte fraction from a complex sample solution (thus leading to an increase in selectivity) and dilution of the sample. As illustrated in Figure 2.9, a gas diffusion unit (GDU) comprises a hydrophobic microporous membrane, such as Teflon or isotactic polypropylene, that separates the donor stream of sample and an acceptor stream of suitable solution. The membrane is permeable to gases. As the donor sample solution is put in contact with the membrane, only species to which the membrane is permeable diffuse into the acceptor solution, which is then subjected to analysis. The gas diffusion process usually requires the addition of an analyte conversion solution to the sample in order to transform ionic analytes to gases. Special attention must be paid to the choice of both the conversion and the acceptor solutions. The conversion solution should provide an efficient and immediate

transformation of analytes to their gaseous forms and an instant reconversion must take place in the acceptor solution.

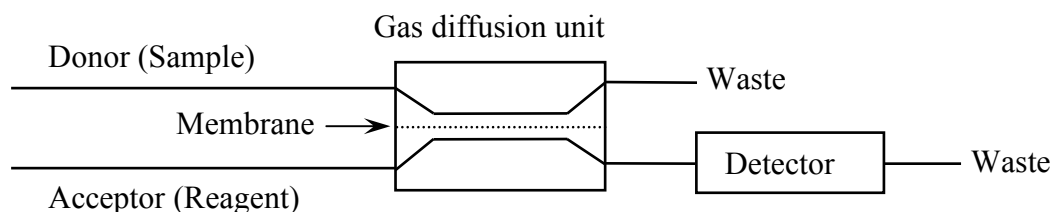


Figure 2.9 A gas diffusion module.

In its simplest form, the gas diffusion in SIA requires a simple manifold in which the donor and acceptor solutions of the gas-diffusion unit are connected to two different ports of the selection valve and the acceptor line is connected to the detector. The sample is aspirated into the holding coil and delivered to the donor port, where gas diffusion to the acceptor solution takes place. Then, the acceptor solution is propelled to the detector. In order to increase the scope of this approach, more complicated manifolds with additional pumps or valves can be constructed. For example, the acceptor stream can be driven by a second pump. The following are some typical applications of gas diffusion for SIA.

M.A. Segundo and A.O.S.S. Rangel developed a sequential injection system with spectrophotometric detection for the determination of free and total sulfur dioxide in wines [18]. The system components were arranged as shown schematically in Figure 2.10. The SIA operating sequence is shown in Table 2.1. It was based on the formation of a color product from the reaction among SO_2 , formaldehyde, and pararosaniline. A GDU was incorporated into the manifold to prevent the wine matrix interference in the spectrophotometric measurement. An acid solution was added to the sample prior to its passage through the donor channel of the GDU to promote gaseous SO_2 formation. In the free SO_2 determination, the sample was directly aspirated into the holding coil. For the total SO_2 determination, the sample was processed after previous in-line hydrolysis of bound SO_2 with an alkali solution.

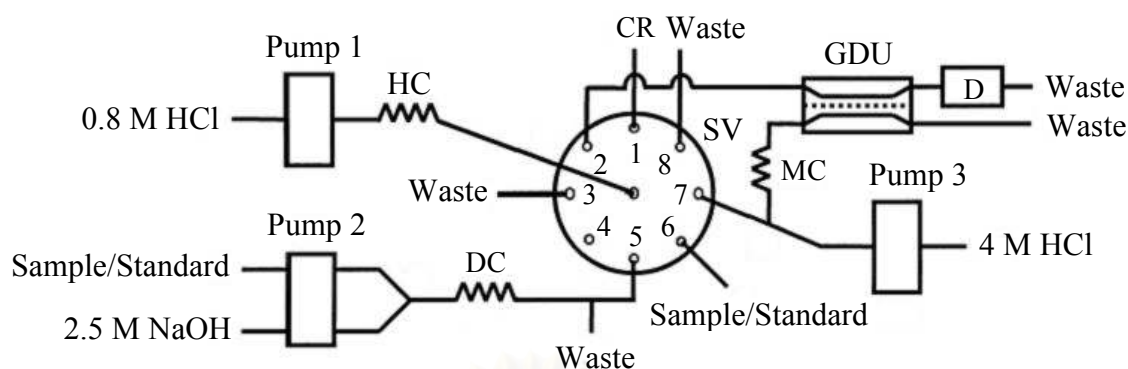


Figure 2.10 SIA manifold for the determination of sulfur dioxide in wines: SV, selection valve; HC, holding coil; DC, dilution coil; MC, mixing coil; D, detection system; CR, color reagent [18].

Table 2.1 Protocol sequence for the determination of sulfur dioxide in wines

Step	SV position	Flow rate ^a (mL min ⁻¹)	Volume (μL)	Description
1	1	1.7	287	Aspirate color reagent
2	2	1.1	185	Propel through acceptor channel of GDU
3	3	4.4	733	Flush holding coil with 0.8 M HCl
4	6/5	1.1/0.6 ^b	190/238 ^b	Aspirate sample or standard
5 ^c	7	0.8	280/210 ^b	Propel through the donor channel of GDU, with addition of 4 M HCl
6	8	4.4	736/445 ^b	Flush holding coil
7	2	2.2	2223	Propel to detector and signal registration
8	7	3.3	1116	Wash donor channel of GDU
9	2	3.3	838	Wash acceptor channel of GDU
10 ^d	5	1.7	112	Wash sample tubing

^a Values of flow rate refer to pump 1.

^b Parameters with different values for determination of free and total SO₂ respectively.

^c The volume of acid added was different for each determination: 83 μL for the determination of free SO₂ and 300 μL for determination of total SO₂.

^d Step executed only for the total SO₂ determination.

R.B.R. Mesquita and A.O.S.S. Rangel described a gas diffusion-sequential injection system with spectrophotometric detection for the determination of free chlorine in waters and bleaches [19]. The manifold for the colorimetric determination of chlorine is depicted in Figure 2.11. The SIA operating sequence is shown in Table 2.2 for chlorine determination in waters and in Table 2.3 for chlorine determination in bleaches. The detection is based on the colorimetric reaction between free chlorine and a low toxicity reagent o-dianisidine. A gas diffusion unit is used to isolate free chlorine from the sample in order to avoid possible interferences. This feature results from the conversion of free chlorine to molecular chlorine (gaseous) with sample acidification.

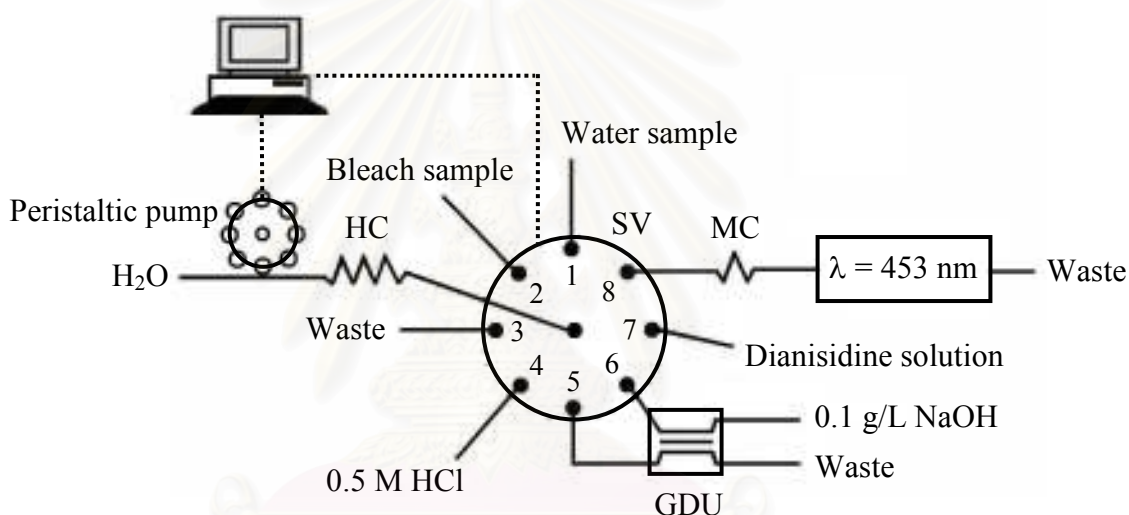


Figure 2.11 Sequential injection manifold for the colorimetric determination of chlorine: HC, holding coil; SV, selection valve; MC, mixing coil.

Table 2.2 Protocol sequence for determination of chlorine in waters

Step	SV position	Flow rate ($\mu\text{L s}^{-1}$)	Volume (μL)	Description
1	4	56	250	Aspirate hydrochloric acid
2	1	56	800	Aspirate sample or standard
3	4	56	250	Aspirate hydrochloric acid
4	1	56	800	Aspirate sample or standard
5	4	56	250	Aspirate hydrochloric acid
6	5	28	2500	Propel through donor channel of GDU
7	6	56	85	Aspirate sample from acceptor channel of GDU
8	7	56	200	Aspirate dianisidine reagent
9	8	56	2800	Propel to detector and signal registration
10	6	56	230	Washing acceptor channel of GDU
11	3	56	400	Washing of holding coil

Table 2.3 Protocol sequence for determination of chlorine in bleaches

Step	SV position	Flow rate ($\mu\text{L s}^{-1}$)	Volume (μL)	Description
1	4	17	25	Aspirate hydrochloric acid
2	2	17	25	Aspirate sample or standard
3	4	17	25	Aspirate hydrochloric acid
4	5	28	150	Propel through donor channel of GDU
5	6	56	85	Aspirate sample from acceptor channel of GDU
6	7	56	200	Aspirate dianisidine reagent
7	8	56	2800	Propel to detector and signal registration
8	6	56	230	Washing acceptor channel of GDU
9	3	56	400	Washing of holding coil

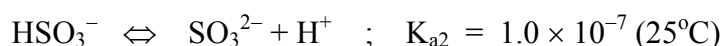
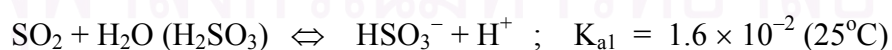
M.T. Oms et al. [20] described an analytical system based on the coupling of gas-diffusion and sequential injection analysis (GD-SIA) and applied to ammonium determination. The sample and an alkaline solution are sequentially aspirated using an automatic burette and mixed by flow reversal while they are being propelled to a GDU. There, the ammonia formed diffuses through a hydrophobic membrane into an acid-base indicator solution. The change in the absorbance of the acid-base indicator solution used as acceptor stream is measured and referred to ammonium content in the sample. The system was applied to the determination of ammonium in environmental samples.

2.4 Sulfites [21,22]

Sulfites in various forms, such as sulfur dioxide, sodium sulfite, sodium bisulfite, potassium bisulfite, sodium metabisulfite, and potassium metabisulfite, are widely used as additives in food and brewing industries. They are used extensively as antimicrobials and to prevent enzymatic and nonenzymatic discoloration in a variety of foods. Sulfur dioxide inhibits yeast, molds, and bacteria; however, yeasts and molds are generally less sensitive to sulfur dioxide than bacteria. Any vegetable or fruit, raw dried, frozen, or canned, that is subject to nonenzymatic or enzymatic browning can benefit by proper treatment with sulfite compounds. Vegetables, such as peas, carrots, beans, cabbage, potatoes, and tomatoes, have more stable color and less deterioration if so treated. Dried fruits held in an atmosphere of sulfur dioxide maintain a more natural appearance.

2.4.1 Forms of Sulfite and Antimicrobial Activity

In aqueous solutions, sulfur dioxide can be written to show the equilibrium:



The distribution of the three forms is dependent upon the pH of the medium as illustrated in Figure 2.12.

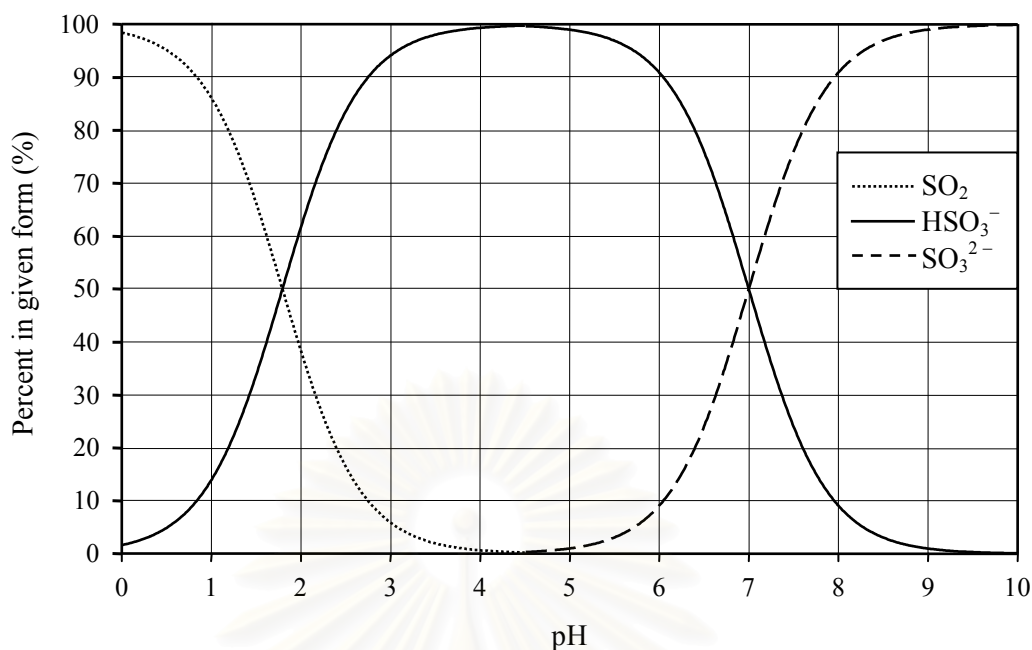


Figure 2.12 The different forms of sulfite at various pH values

Bisulfite (HSO_3^-) is a predominant form in the intermediate pH range. Sulfur dioxide, the predominate moiety at low pH, is a gas that is used for fumigation. The sulfite salts are generally used in aqueous solutions that are used as dips or sprays for foods.

The pH is the most important factor impacting the antimicrobial activity of sulfites. The inhibitory effect of sulfites is most pronounced when the acid or $\text{SO}_2 \cdot \text{H}_2\text{O}$ is in the undissociated form. Therefore the most effective pH range is less than 4.0. King et al. [23] proved this when they found that undissociated H_2SO_3 ($\text{SO}_2 \cdot \text{H}_2\text{O}$) was the only form active against yeast and that neither HSO_3^- nor SO_3^{2-} had antimicrobial activity. Similarly, $\text{SO}_2 \cdot \text{H}_2\text{O}$ was shown to be 1000, 500, and 100 times more active than HSO_3^- or SO_3^{2-} against *E. coli*, yeast, and *Aspergillus niger*, respectively [24]. Increased effectiveness at low pH likely is due to the fact that unionized sulfur dioxide can pass across the cell membrane in this form.

Sulfites, especially as HSO_3^- , are very reactive. These reactions not only determine the mechanism of action of the compounds, they also influence antimicrobial activity. For example, sulfites form addition compounds (α -hydroxysulfonates) with aldehydes and ketones. These addition compounds are in equilibrium in solution with free sulfite ions, resulting in the formation of a thiol (R-

SH) and S-substituted thiosulfates (R-S-SO₃⁻). It is generally agreed that these bound forms have much less or no antimicrobial activity compared to the free forms.

2.4.2 Sulfites Allergies

The toxic effect of sulfur dioxide in humans is variable. Some persons may tolerate up to 50 mg kg⁻¹ body weight, while others have headache, nausea, and diarrhea. Asthmatics and people with allergies to aspirin (also known as salicylate sensitivity) are at an elevated risk for reaction to sulfites. The reaction can be fatal and requires immediate treatment at an emergency room, and can include sneezing, swelling of the throat, and hives. Those who are allergic to sulfites are urged to avoid products that could contain them.

2.4.3 Amounts in Food and Regulations

Sulfites are considered GRAS (generally recognized as safe) substances by the Food and Drug Administration (FDA) when used in amounts that are in accordance with good manufacturing practices. They are allowed in fruit juices and concentrates, dehydrated fruits and vegetables, and wine. The amounts of sulfite used in foods and beverages vary greatly between countries. An estimate of the concentrations of sulfites used in foods as an antimicrobial was illustrated in Table 2.4 [25]. Due to its allergenic effect on hypersensitive people, the sulfite content in foods has been strictly limited. Products containing sulfite more than the established threshold level must be adequately labeled. For example, in the United States, the FDA has required labeling of products containing more sulfite than 10 mg L⁻¹.

สถาบันวิทยบริการ
จุฬาลงกรณ์มหาวิทยาลัย

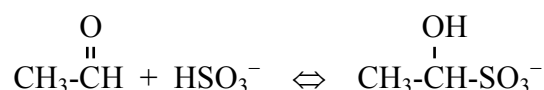
Table 2.4 Applications of sulfites in foods as antimicrobials and the concentrations used

Food	Use Concentration (mg kg ⁻¹ SO ₂) ^a
Beer	10 – 30
Fresh fruits	100
Fresh vegetables (onion, garlic, horseradish)	50 – 1000
Fruit juices	10 – 100
Fruit-based sauces and related products	50 – 100
Fruit pulps, purees, and fillings	50 – 500
Jams and jellies	50 – 100
Nonalcoholic beverages	20 – 200
Sausage	450
Vinegar	50 – 200
Wine	100 – 300

^a Sulfites are allowed only in certain foods in different countries, and concentration varies by country.

2.4.4 Sulfur Dioxide in Wine [18,26]

Sulfur dioxide is added to wine during its production to prevent undesirable microbial growth and oxidation processes. In wine, sulfur dioxide can exist in a variety of free and bound states as illustrated in Figure 2.13. A portion of the sulfur dioxide bound with compounds in the wine is called bound sulfur dioxide. The remainder is called free sulfur dioxide. Total sulfur dioxide is the sum of free and bound sulfur dioxide. Most of the free ionic sulfur dioxide occurs as bisulfite ions (HSO₃⁻). Only a small portion of the total sulfur dioxide content exists as free dissolved gas (SO₂). An additional small fraction exists as free sulfite ions (SO₃²⁻). Because sulfur dioxide binds readily with several constituents in wine, it often occurs as hydroxysulfonates. Much of this is reversibly associated with acetaldehyde. The reaction for the binding of acetaldehyde and HSO₃⁻ is shown below.



Bisulfite addition products also form with anthocyanins, tannins, pyruvic acid, α -ketoglutarate, sugars, and sugar acids.

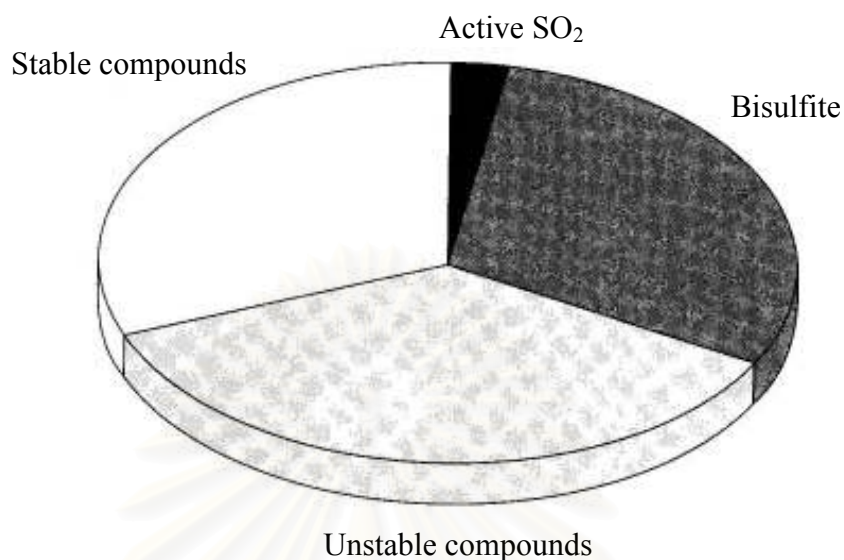


Figure 2.13 Relative proportions of the various forms of sulfur dioxide in wine

The determination of sulfur dioxide is routinely performed in wines for different reasons. During production, the SO_2 level must be controlled to avoid high concentrations, which give wines a disagreeable aroma and taste and also inhibits malolactic fermentation. The SO_2 concentration must also be monitored and adjusted before bottling, since losses by diffusion, oxidation and binding occur during wine ageing. Finally, the SO_2 concentration is also determined in the final product, since its maximum value is established by legislation in several countries. In order to determine the total SO_2 in wine, acid or base hydrolysis is necessary to release S(IV) bound as carbonyl adducts or sulfonates.

2.4.5 Methods for Sulfite/Sulfur Dioxide Determination

The method for sulfite determination is of great importance for food assurance and quality control. The classical Monier-Williams method [27] for the determination of sulfite involves its distillation under an inert atmosphere (e.g. nitrogen). The analyte is collected in a hydrogen peroxide solution producing sulfuric acid, which can be determined in the conventional way. In spite of its general applicability and accuracy, the long time required for the analysis precludes a more extensive use of the Monier-Williams method, especially in routine analysis. Other

developed methods for sulfite determination include spectrophotometry [28], spectrofluorimetry [29,30], chemiluminescence [31], electrochemistry [32,33], chromatography [34,35], and capillary electrophoresis [36,37].

Flow injection analysis (FIA) and sequential injection analysis (SIA) which can be automated and used for a broad range of samples with high sampling frequency have also been applied to determine sulfite and sulfur dioxide. To improve selectivity, a gas diffusion unit (GDU) has been incorporated in some flow systems to separate the liberated sulfur dioxide from sample matrices [18,38-43]. Spectrometric and electrochemical detection are often coupled to flow systems for sulfite/sulfur dioxide determination. Spectrophotometric, fluorimetric, and chemiluminescence detection can be performed after mixing with some reagents, which results in cost and complication of the analysis as well as the toxicity of certain reagents. Electrochemical detection is an attractive option due to the direct electrochemical oxidation of sulfite. The following are typical applications of flow-analysis techniques for the sulfite/sulfur dioxide determination.

L.G. Decnop-Weever and J.C. Kraak [39] developed a GD-FIA with spectrophotometric detection for the determination of sulfite in wines. The method is based on the change of the absorbance of an indicator solution when sulfur dioxide, liberated from the matrix, diffuses via a permeable membrane into the indicator solution of bromocresol green and locally shifts the pH. The method is applicable in the range of 1-20 mg L⁻¹ for sulfite and the lower limits of detection is 0.1 mg L⁻¹. Carbon dioxide interfere the measurement and therefore the method cannot be used for sparkling wines and beers.

M.A. Segundo and A.O.S.S. Rangel [18] developed a GD-SIA with spectrophotometric detection for the determination of free and total sulfur dioxide in wines. It was based on the formation of a colored product from the reaction among SO₂, formaldehyde and *p*-rosaniline. For the free SO₂ determination, the sample was directly aspirated into the holding coil; for the total SO₂ determination, the sample was processed after previous in-line hydrolysis of bound SO₂ with an alkali solution. Two second-order calibration curves were established, defining two concentration ranges: 2–40 mg L⁻¹ for the free SO₂ determination and 25–250 mg L⁻¹ for the total SO₂ determination. The sample frequency was about 16 h⁻¹. This system is far from ideal, since pararosaniline is carcinogenic and its reaction with sulfur dioxide is rather slow.

H. Mana and U. Spohn [41] developed a GD-FIA with fluorimetric detection for the determination of sulfite/hydrogen sulfite/sulfur dioxide on the basis of an in situ-generated *o*-phthalaldehyde (OPA)/ammonium reagent. The highest sensitivity was achieved at an excitation wavelength of 330 nm, an emission wavelength of 390 nm, and at pH 6.5. Sulfite concentrations between 40 nM and 0.1 mM can be determined by utilization of a reagent that contains 0.2 mM OPA and 0.4 M NH₄Cl in 50 mM potassium phosphate buffer. After 1000-fold dilution, the total sulfite content can be determined in white and red wines.

J.M. Lin and T. Hobo [38] described a GD-FIA with chemiluminescent detection for selective determination of sulfite. The light accompanying the reaction between sodium carbonate and copper (II) mixture solution with sulfite is detected. The concentration of sulfite is proportional to the chemiluminescence intensity in the range of $1.0 \times 10^{-6} - 5 \times 10^{-4} \text{ mol L}^{-1}$. The limit of detection is $5 \times 10^{-7} \text{ mol L}^{-1}$. This method has been successfully applied to the determination of sulfite in wines.

R. Carballo et al. [44] described a FIA with amperometric detection using Poly[Ni-(protoporphyrin IX)] film at submonolayer-level-modified glassy carbon electrodes for quantification of both free and total SO₂. The method gives a linear range up to 9.0 mg mL^{-1} and a detection limit of 0.15 mg mL^{-1} for SO₂.

T.J. Cardwell and M.J. Christophersen [40] described a GD-FIA for the simultaneous determination of ascorbic acid (AA) and sulfur dioxide in red and white wines and various fruit juices. The flow injection manifold consists of a dual channel amperometric detection system, where AA is detected at a glassy carbon electrode and sulfur dioxide is detected at a platinum electrode after separation by a GDU. In the application of this method to the analysis of both analytes in wines and fruit juices, the results for white wines, fruit juices and juice concentrates agree well with data obtained by ion-exclusion chromatography. However, in the case of red wines and a sweet white wine, it is necessary to extract the analytes using solid phase extraction on a quaternary amine SAX cartridge before acceptable results are achieved by the method. The linear dynamic range for AA is $3-50 \text{ mg L}^{-1}$ with a detection limit of 1.5 mg L^{-1} and for sulfur dioxide the linear range is $0.25-15 \text{ mg L}^{-1}$ with a detection limit of 0.05 mg L^{-1} . The sampling frequency for both analytes is 30 h^{-1} .

CHAPTER III

EXPERIMENTAL

3.1 Apparatus

The following is the list of apparatus used in this work.

- 3.1.1 PalmSens (Palm Instrument BV, Houten, The Netherlands)
- 3.1.2 Single-compartment, three-electrode glass cell (Custom made)
- 3.1.3 BDD electrode (Toyo Kohan Co., Ltd., Japan)
- 3.1.4 Glassy carbon disk electrode, ϕ 3 mm (CH Instrument, USA)
- 3.1.5 Ag/AgCl reference electrode for CV (CH Instrument, USA)
- 3.1.6 Platinum wire, ϕ 0.2 mm (Goodfellow, USA)
- 3.1.7 Syringe pump (Cavro XL 3000, Cavro Scientific Instruments Inc., USA) with a 2.5 ml syringe
- 3.1.8 Six port selection valve (Cavro Smart Valve, Cavro Scientific Instruments Inc., USA)
- 3.1.9 Peristaltic pump (SMP-23, EYELA, Japan)
- 3.1.10 Electrochemical flow cell (Bioanalytical Systems Inc., USA)
- 3.1.11 Ag/AgCl reference electrode for SIA (Bioanalytical Systems Inc., USA)
- 3.1.12 Gas diffusion unit (Custom made)
- 3.1.13 pH meter (Metrohm 744 pH meter, Metrohm, Switzerland)
- 3.1.14 Analytical balance (Mettler AT 200, Mettler, Switzerland)
- 3.1.15 Ultrasonic bath (ULTRASONIK 28H, ESP Chemicals, Inc., USA)

สถาบันวิทยบริการ
จุฬาลงกรณ์มหาวิทยาลัย

3.2 Chemicals

All chemicals used in this work were analytical grade. List of chemicals and their suppliers are shown in Table 3.1.

Table 3.1 List of chemicals and their suppliers

Chemicals	Suppliers
di-Sodium hydrogen phosphate dihydrate	Merck (Darmstadt, Germany)
Ethylenediaminetetraacetic acid disodium salt dihydrate	Riedel-de Haën (Seelze, Germany)
Formaldehyde 38 %	BDH (Poole, England)
Iodine	Merck (Darmstadt, Germany)
ortho-Phosphoric acid 85 %	Merck (Darmstadt, Germany)
Potassium dihydrogen orthophosphate	BDH (Poole, England)
Potassium iodide	BDH (Poole, England)
Sodium hydrogen carbonate	BDH (Poole, England)
Sodium dodecyl sulfate	Sigma (St. Louis, USA)
Sodium hydroxide	Merck (Darmstadt, Germany)
Sodium sulfite	Merck (Darmstadt, Germany)
Sodium thiosulphate pentahydrate	BDH (Poole, England)
Starch	BDH (Poole, England)
Sulfuric acid 95–97 %	Merck (Darmstadt, Germany)

3.3 Preparation of Solutions

The followings include the preparation procedures of standard solutions and other solutions employed in this work.

3.3.1 Reagents Used in Cyclic Voltammetry

A 1 mM sodium sulfite was prepared by dissolving 0.0063 g of sodium sulfite in 50 mL of phosphate buffer solution.

The phosphate buffer solutions (pH 5–9) were prepared from 0.1 M potassium dihydrogen orthophosphate and 0.1 M disodium hydrogen orthophosphate. A phosphate buffer (pH 4) was prepared from 0.1 M potassium dihydrogen orthophosphate and the pH was adjusted with 85% orthophosphoric acid. A phosphate buffer (pH 10) was prepared from 0.1 M disodium hydrogen orthophosphate with pH adjustment using 0.1 M sodium hydroxide.

3.3.2 Reagents Used in Sequential Injection Analysis

A stock solution of $\sim 500 \text{ mg L}^{-1}$ sulfite (SO_3^{2-}) was prepared daily by dissolving 0.0394 g of Na_2SO_3 in 50 mL of 1 g L^{-1} EDTA solution as a stabilizing agent [45]. The stock solution was standardized by iodimetric titration.

A stock solution of $\sim 500 \text{ mg L}^{-1}$ sulfur dioxide (SO_2) was prepared daily by dissolving 0.0492 g of Na_2SO_3 in 50 mL of 1 g L^{-1} EDTA solution and standardized by iodimetric titration. The stock solution of sulfur dioxide is usually prepared by dissolving the sodium sulfite [18,45,46] because the solution of sulfite generates sulfur dioxide in the acidic solution as shown in Figure 2.12.

The working standard solutions of sulfite were obtained by diluting the stock solution in 1 g L^{-1} EDTA solution.

A H_2SO_4 solution (2 M) was prepared by diluting 55.5 mL of 95–97% H_2SO_4 to 500 mL with deionized water.

The carrier solution for the SI system consisted of a 0.1 M phosphate buffer solution (pH 8) containing 0.1% (w/v) sodium dodecyl sulfate.

3.3.2 Reagents Used in Iodimetric Titration

A 0.01 M iodine solution was prepared by dissolving 1.27 g of iodine into 500 mL deionized water containing 10 g of potassium iodide. The concentration of iodine was determined by titration with the secondary standard solution of 0.1 M sodium thiosulfate.

A 25% (v/v) H_2SO_4 solution was prepared by diluting 125 mL of 95–97% H_2SO_4 to 500 mL with deionized water.

A 1 M sodium hydroxide was prepared by dissolving 40 g of NaOH pellets in 1 L of deionized water.

3.4 Cyclic Voltammetry

The cyclic voltammetry measurements were performed in a single-compartment, three-electrode glass cell as illustrated in Figure 3.1. A BDD electrode, an Ag/AgCl with a salt bridge and a platinum wire were used as the working electrode, the reference electrode and the counter electrode, respectively. The BDD electrode was pressed against an O-ring (area 0.07 cm^2) at the bottom of the cell. Ohmic contact was made by placing a brass plate on the backside of the Si substrate of the BDD electrode. The cell was housed in a faradaic cage to reduce the electronic noise. The electrochemical measurements were recorded using a PalmSens.

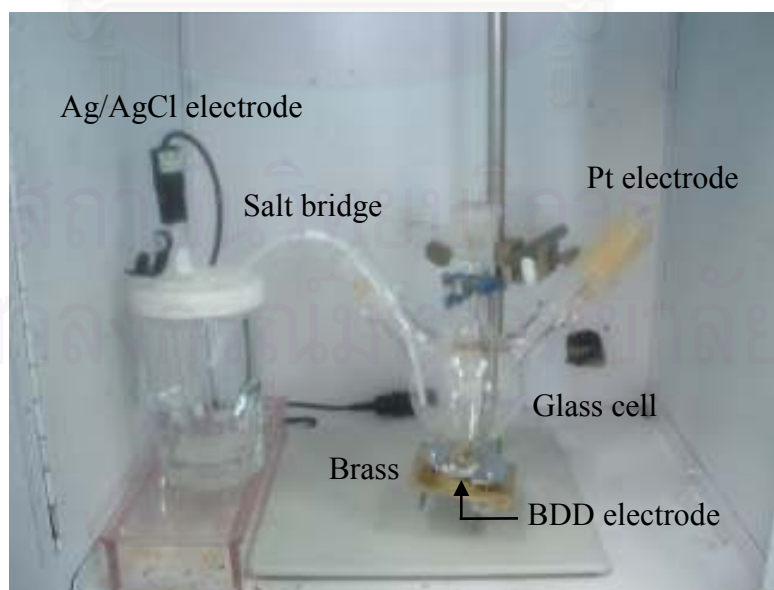


Figure 3.1 The electrochemical cell for cyclic voltammetry experiment.

3.4.1 pH Dependence

The influence of pH on the electrochemical response of sulfite at BDD electrode was studied by cyclic voltammetry. Solutions of 1 mM sodium sulfite in 0.1 M phosphate buffer at pH 4, 5, 6, 7, 8, 9 and 10 were prepared. The potential was scanned from 0 to 1.2 to 0 V at a scan rate of 50 mV s^{-1} .

3.4.2 Comparison of BDD Electrode with Glassy Carbon Electrode

The glassy carbon (GC) electrode is a very common electrode used in voltammetry. It was used in this experiment for comparison to the BDD electrode. The electrochemical oxidation of sulfite at the BDD electrode and the GC electrode were investigated by cyclic voltammetry. The 0.1 M phosphate buffer solution and 1 mM sodium sulfite in 0.1 M phosphate buffer solution were prepared. The pH 8 of buffer solution was chosen from the previous experiment in Section 3.4.1 for the experiment. The potential was scanned from 0 to 1.2 to 0 V for the BDD electrode and 0 to 1.1 to 0 V for the GC electrode. The scan rate of 50 mV s^{-1} was used. The results obtained from cyclic voltammograms for both electrodes were compared.

3.4.3 The Scan Rate Dependence Study

The effect of the scan rate on the electrochemical behaviors of sulfite was investigated by variation of the scan rate in cyclic voltammetry. The solutions of 1 mM Na_2SO_3 in 0.1 M phosphate buffer (pH 8) were prepared. The potential was scanned from 0 to 1.2 to 0 V at a scan rate of 10, 25, 50, 100, 200, and 300 mV s^{-1} . The peak currents obtained from cyclic voltammogram at each scan rate were plotted as a function of the square root of the scan rate.

3.5 Sequential Injection with Amperometric Detection

For sequential injection analysis with amperometric detection, the SIA system consisted of a syringe pump with a 2.5 mL syringe, a six port selection valve, a gas diffusion unit, a peristaltic pump, an electrochemical flow cell, and a potentiostat (PalmSens). The system components were arranged as shown schematically in Figure 3.2. All tubing connecting the different components of the flow system was PTFE with the inner diameter of 0.8 mm. The GDU shown in Figure 3.3 consisted of two symmetric acrylic blocks, two silicone gaskets with a channel (31 mm long, 1.5 mm

wide and 0.2 mm thick) as the spacer and a PTFE hydrophobic membrane. The membrane was placed between two silicone gaskets which were sandwiched between two acrylic blocks. Two acrylic blocks were pressed against each other by four screws. The electrochemical flow cell shown in Figure 3.4 consisted of a silicone gasket (0.5 mm thick) as a spacer (area 0.3 cm²), the boron-doped diamond working electrode, the Ag/AgCl reference electrode, and the stainless steel tube counter electrode.

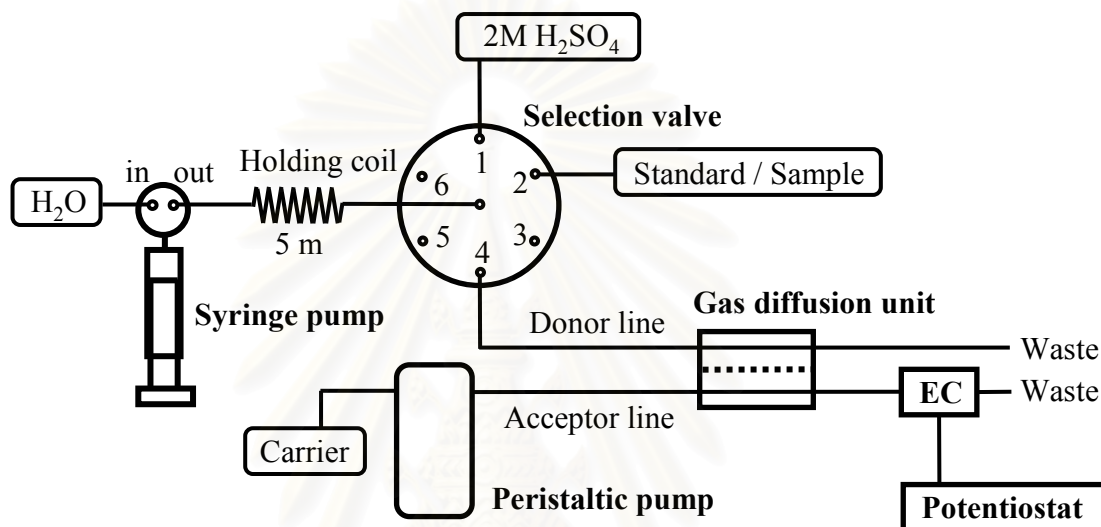


Figure 3.2 The SIA manifold for the determination of sulfite: EC, electrochemical flow cell.



Figure 3.3 The gas diffusion unit

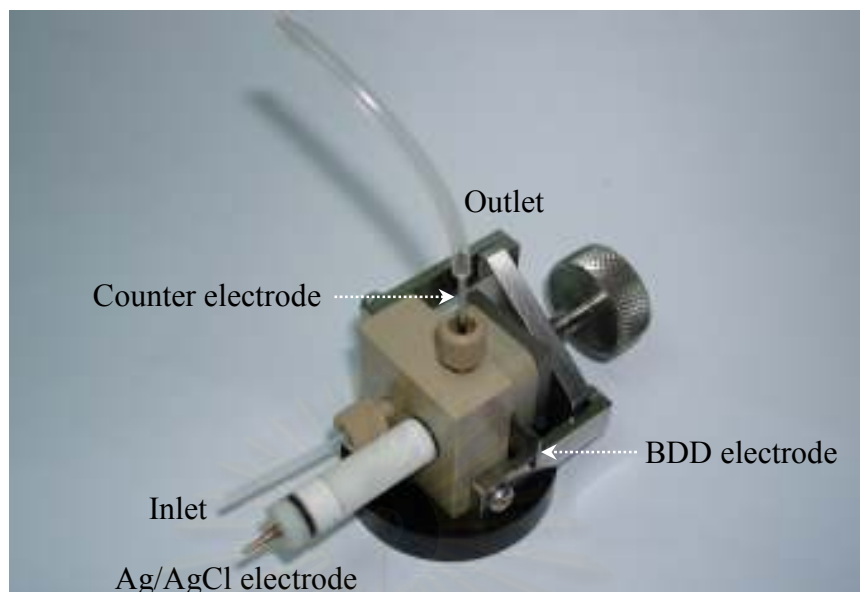


Figure 3.4 The electrochemical flow cell

The carrier, 0.1 M phosphate buffer (pH 8)/0.1% SDS, was passed through the electrochemical flow cell by a peristaltic pump. The operating sequence of the SIA system for the analysis of sulfite is listed in Table 3.2. The analytical cycle started with the aspiration of water into the syringe. Next, the sulfuric acid and the standard/sample solution were aspirated into the holding coil in which the gaseous sulfur dioxide was generated. The flow was then reversed and the mixture was propelled through the donor channel of the GDU. During this step, the generated sulfur dioxide diffused through the membrane into the carrier solution in the acceptor channel of the GDU. Then, the sulfite formed in the phosphate buffer (pH 8)/0.1% SDS carrier was carried to the electrochemical flow cell and detected directly at the BDD electrode.

Table 3.2 The SIA operating sequence for sulfite analysis

Step	Operation	Valve of pump	Port of SV ^a	Volume (μL)	Flow rate ($\mu\text{L s}^{-1}$)
1	Aspirate water to syringe pump	in	–	600	100
2	Aspirate 2 M H_2SO_4 to holding coil	out	1	100	50
3	Aspirate standard/sample to holding coil	out	2	50	50
4	Dispense mixture to donor channel of GDU	out	4	750	25

^a SV is selection valve

3.5.1 Optimum Potential for Amperometric Detection

In order to obtain the optimal potential for amperometric detection in the sequential injection (SI) system, the hydrodynamic voltammetry was performed by varying applied potentials from 0.70 V to 1.05 V at intervals of 0.05 V. In the proposed SI system, the background currents of the carrier (0.1 M phosphate buffer (pH 8)/0.1% SDS) and the signal currents for four consecutive injections of 10 mg L^{-1} sulfite were measured at each potential respectively. Then the average background currents and the average peak currents obtained from the hydrodynamic voltammogram were plotted as a function of applied potential.

3.5.2 Effect of Sodium Dodecyl Sulfate

The preliminary experiment using the proposed SI system revealed that electrode fouling occurred at the BBD electrode in the amperometric detection of sulfite. This experiment was performed to show that the electrode fouling problem can be solved by adding the sodium dodecyl sulfate (SDS) in the carrier solution of 0.1 M phosphate buffer (pH 8). Carrier solutions of 0.1 M phosphate buffer (pH 8) and 0.1 M phosphate buffer (pH 8)/0.1% SDS were prepared. The signal currents for fifteen consecutive injections of 10 mg L^{-1} sulfite were measured for each carrier and the results were compared.

3.5.3 Sequential Injection Parameters

In the SIA operating sequence, the volume of sulfite solution was set at 50 μL . The concentration of 2 M for sulfuric acid was adopted from a study in a previous work [46]. In order to minimize sample dispersion, the length of the connection between the selection valve and the donor channel of the GDU was set at 15 cm and the length of the connection between the acceptor channel of the GDU and the electrochemical flow cell was set at 20 cm. The sequence of sulfite and acid aspiration was first investigated. Then the volume of 2 M H_2SO_4 was optimized. Finally the flow rate for propelling the acidified sample to the GDU and the flow rate of carrier were optimized respectively.

3.5.3.1 Sequence of Sulfite and Acid Aspiration

The order of the sulfite and acid aspiration in the SIA experiment was investigated. Two SIA operating sequences were used. One (Table 3.2) was the sulfite aspiration after the acid aspiration and the other (Table 3.3) was the acid aspiration after the sulfite aspiration. Concentrations of sulfite used for the experiment were 10 mg L^{-1} and 50 mg L^{-1} . The signal current for four consecutive injections of sulfite was measured. The results were compared to obtain the optimal sequence of the sulfite and acid aspiration.

Table 3.3 The SIA operating sequence for sulfite analysis. The acid was aspirated after sulfite aspiration

Step	Operation	Valve of pump	Port of SV	Volume (μL)	Flow rate ($\mu\text{L s}^{-1}$)
1	Aspirate water to syringe pump	in	–	600	100
2	Aspirate standard/sample to holding coil	out	2	50	50
3	Aspirate 2 M H_2SO_4 to holding coil	out	3	100	50
4	Dispense mixture to donor channel of GDU	out	4	750	25

3.5.3.2 Volume of Sulfuric Acid

The volume of 2 M H₂SO₄ in the SIA operating sequence (Step 2 in Table 3.2) was investigated over the range 20–140 μL at intervals of 20 μL. The signal currents for four consecutive injections of 10 mg L⁻¹ and 50 mg L⁻¹ sulfite were measured for each volume of 2 M H₂SO₄. The concentration of 10 mg L⁻¹ was in the linear concentration range and the concentration of 50 mg L⁻¹ was over the linear concentration range. The concentration of 50 mg L⁻¹ was used to be sure that the optimum volume of acid is enough for sulfur dioxide generation to this concentration. The peak currents obtained from the SIA with amperometric detection results were used to find the optimal volume. Aspiration of another plug of 2 M H₂SO₄ after sulfite aspiration as shown in Table 3.4 was also studied over the range 0–60 μL at intervals of 20 μL.

Table 3.4 The SIA operating sequence for analysis of sulfite. Another plug of acid was aspirated after sulfite aspiration

Step	Operation	Valve of pump	Port of SV	Volume (μL)	Flow rate (μL s ⁻¹)
1	Aspirate water to syringe pump	in	–	600	100
2	Aspirate 2 M H ₂ SO ₄ to holding coil	out	1	100	50
3	Aspirate standard/sample to holding coil	out	2	50	50
4	Aspirate 2 M H ₂ SO ₄ to holding coil	out	3	0–60	0–60
5	Dispense mixture to donor channel of GDU	out	4	750–810	25

3.5.3.3 Propelling Flow Rate

The flow rate for propelling the acidified sample to the donor channel of the GDU (Step 4 in Table 3.2) was investigated in the range 10–35 μL s⁻¹

at intervals of $5 \mu\text{L s}^{-1}$. The signal currents for four consecutive injections of 10 mg L^{-1} sulfite were measured for each flow rate. The peak currents obtained from the SIA with amperometric detection results were used to find the optimal flow rate.

3.5.3.4 Flow Rate of Carrier

The flow rate of carrier for carrying sulfite to the electrochemical flow cell was studied in the range $0.25\text{--}1.0 \text{ mL min}^{-1}$ at intervals of 0.25 mL min^{-1} . The signal currents for four consecutive injections of 10 mg L^{-1} sulfite were measured for each flow rate. The peak currents obtained from the SIA with amperometric detection results were used to find the optimal flow rate.

3.5.4 Influence of Sample volume

The sample volume was studied in the range $10\text{--}50 \mu\text{L}$ at intervals of $10 \mu\text{L}$. The signal currents for four consecutive injections of 10 mg L^{-1} sulfite were measured for each volume. The peak currents were obtained from the SIA with amperometric detection results.

3.5.5 Linearity

A stock solution of $\sim 500 \text{ mg L}^{-1}$ sulfite was freshly prepared and standardized by iodimetric titration. Then a portion of stock solution was diluted to a concentration range from 0.2 to 50 mg L^{-1} sulfite. The signal currents for four consecutive injections of sulfite were measured for each concentration. The peak currents obtained from the SIA with amperometric detection results were used to plot the calibration curve and the linear range can be obtained.

3.5.6 Limit of Detection

The limit of detection for sulfite was examined by four consecutive injections of low concentrations of sulfite under the optimal parameters. The concentration of sulfite was in the range $0\text{--}0.2 \text{ mg L}^{-1}$. The limit of detection was determined as the concentration of sulfite that provided the peak current three times the noise ($S/N = 3$).

3.5.7 Repeatability

The repeatability was studied by ten consecutive injections of 10 mg L^{-1} sulfite and the signal current was measured. The peak currents obtained from the SIA with amperometric detection results were used to calculate the relative standard deviation (%RSD).

3.6 Real Sample Analysis

The proposed SIA method was applied to the determination of free and total sulfur dioxide in wine samples. The analytical results were compared with those obtained by iodimetric titration which was used in many previous works for comparison.

3.6.1 Effect of Ethanol

Most wine samples contain the ethanol about 10–14 % (v/v). Thus the effect of ethanol was studied by varying the content of ethanol in the standard solution of sulfite from 0 to 14 % at intervals of 2 %. The signal currents for four consecutive injections of 10 mg L^{-1} sulfite solution containing various content of ethanol were measured.

3.6.2 Determination of Sulfur Dioxide in Wines by Developed SIA

The external standard method was used to determine the amount of free and total sulfur dioxide in wines. A stock solution of $500 \text{ mg L}^{-1} \text{ SO}_2$ was freshly prepared. Working solutions of $5\text{--}30 \text{ mg L}^{-1} \text{ SO}_2$ containing 10 % ethanol were prepared from the stock solution. The SIA operating sequence listed in Table 3.2 was used for the preparation of the calibration curve and the determination of sulfur dioxide in wines. However, the standard/sample volume was reduced to $15 \mu\text{L}$ in order to perform the SIA analysis in the linear concentration range of sulfur dioxide. The experiments were carried out by four consecutive injections of standard/samples. Results of working solutions were used to plot the calibration curve.

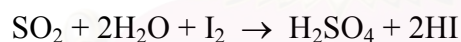
In the SIA analysis of free sulfur dioxide, the sample was directly aspirated into the holding coil. For the total sulfur dioxide determination, 2 mL of sample was first treated with 2.5 mL of 1 M NaOH to release the bound sulfur

dioxide. The mixture was then acidified with 1 mL of 25% (v/v) H₂SO₄. After 10 minute, 1 mL of absolute ethanol was added to the mixture and diluted to 10 mL with 0.1 g L EDTA solution. Then the mixture was rapidly analyzed.

3.6.3 Determination of Sulfur Dioxide in Wines by Iodimetric Titration [47]

In the iodimetric determination of free SO₂, 50 ml of sample was treated with 5 mL of 25% (v/v) H₂SO₄, and next with 1 g of NaHCO₃ and 1% starch solution. Titration with standardized I₂ solution was then carried out rapidly. The end point was indicated by a blue color, which persisted for at least 30 seconds. For the iodimetric determination of total SO₂, 20 mL of sample was initially treated with 25 mL of 1 M NaOH, in order to release the bound sulfur dioxide. Samples were then acidified with 10 mL of 25% H₂SO₄ and rapidly titrated. Since several matrix compounds in wine interfere with iodimetric analysis, correction of iodine consumption [46] must be applied. The same amount of wine was first treated with formaldehyde, forming the methanesulfonate adduct, before titration with iodine. The amount of iodine consumed gives the amount of non-sulfite reducer in the sample.

The reaction which occurred in the iodimetric titration for sulfur dioxide is shown below.



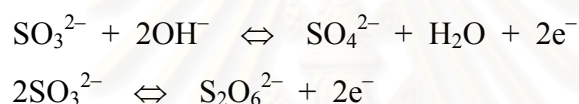
CHAPTER IV

RESULTS AND DISCUSSION

4.1 Cyclic Voltammetry Measurement

4.1.1 pH Dependence

The effect of pH on the electrochemical response of sulfite at BDD electrode was studied by cyclic voltammetry. Cyclic voltammograms of sulfite and phosphate buffer solutions at pH 4, 5, 6, 7, 8, 9, and 10 are shown in Figure 4.1. The electrochemical data of sulfite obtained from cyclic voltammograms are summarized in Table 4.1. The anodic oxidation of sulfite can be expressed by the following equations [48]:



The production of dithionate ion can be neglected according to the literature [49].

It was observed that sulfite gave well-defined cyclic voltammograms in neutral and alkali solutions. In the acidic solution, the oxidation peak potential shifted to more positive values as the pH of solutions decreased. This result indicates that the oxidation of sulfite in the acidic solution is more difficult than that in neutral and alkali solutions, which corresponds to the equation for anodic oxidation of sulfite to sulfate. It was also observed that in alkali solutions, sulfite provided the highest peak current at pH 8 while the oxidation peak potentials were almost equal. Therefore pH 8 was chosen as the optimum pH of the phosphate buffer solution for the electrochemical oxidation of sulfite.

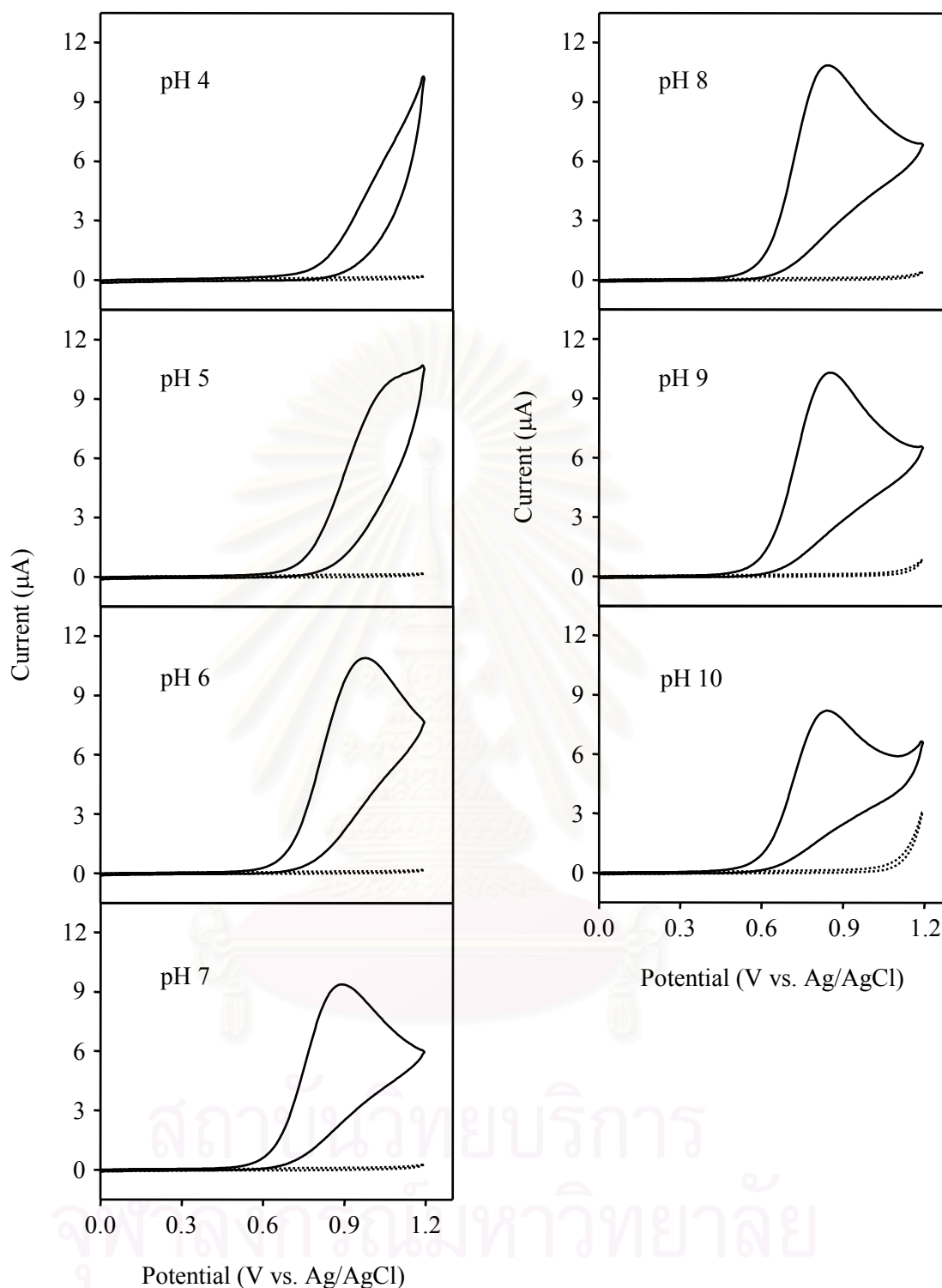


Figure 4.1 Cyclic voltammograms of 1 mM Na_2SO_3 in 0.1 M phosphate buffer solution (solid line) at pH 4, 5, 6, 7, 8, 9 and 10 for the BDD electrode. Cyclic voltammograms of 0.1 M phosphate buffer solution (dash line) are also shown. The scan rate was 50 mV s^{-1} . The area of electrode was 0.07 cm^2 .

Table 4.1 Comparison of electrochemical data obtained from cyclic voltammograms of 1 mM sodium sulfite at pH 4, 5, 6, 7, 8, 9, and 10

pH	E_{pa} (V vs. Ag/AgCl)	i_{pa} (μ A)
4	–	–
5	1.079	9.864
6	0.983	10.769
7	0.896	9.268
8	0.851	10.742
9	0.857	10.196
10	0.851	8.041

4.1.2 Comparison of BDD Electrode with Glassy Carbon Electrode

The electrochemical oxidation of sulfite and phosphate buffer solution (pH 8) at the BDD electrode and the glassy carbon (GC) electrode were investigated by cyclic voltammetry. Cyclic voltammograms of 1 mM sodium sulfite in 0.1 M phosphate buffer solution (pH 8) at the BDD electrode and the GC electrode are shown in Figure 4.2. Cyclic voltammograms of 0.1 M phosphate buffer solution (pH 8) as the background at the BDD electrode and the GC electrode are shown in Figure 4.3. It was observed that the well-defined irreversible cyclic voltammograms were obtained for both electrodes. However the background current for the BDD electrode was about eight times smaller than that for the GC electrode and the peak current for the BDD electrode is slightly higher than that for the GC electrode. Thus the higher sensitivity was obtained for the BDD electrode, compared to the GC electrode.

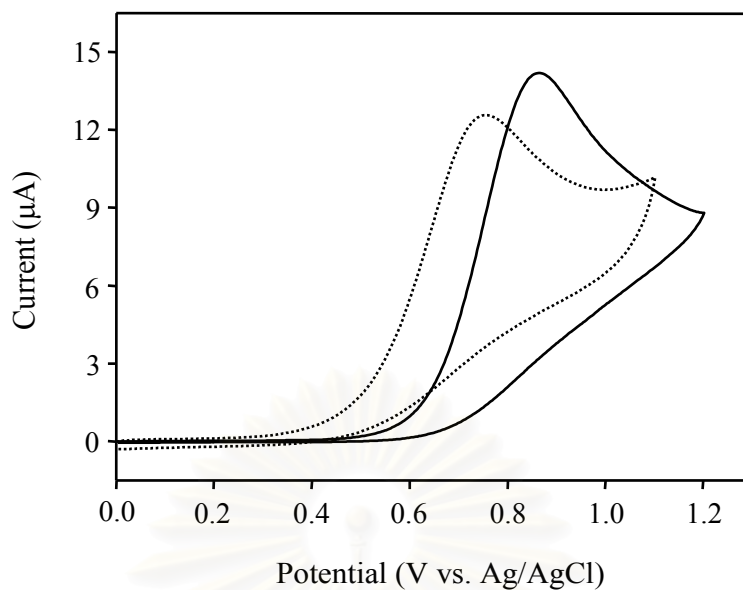


Figure 4.2 Cyclic voltammograms of 1 mM Na_2SO_3 in 0.1 M phosphate buffer solution (pH 8) at the BDD electrode (solid line) and the GC electrode (dash line). The scan rate was 50 mV s^{-1} . The area of electrode was 0.07 cm^2 .

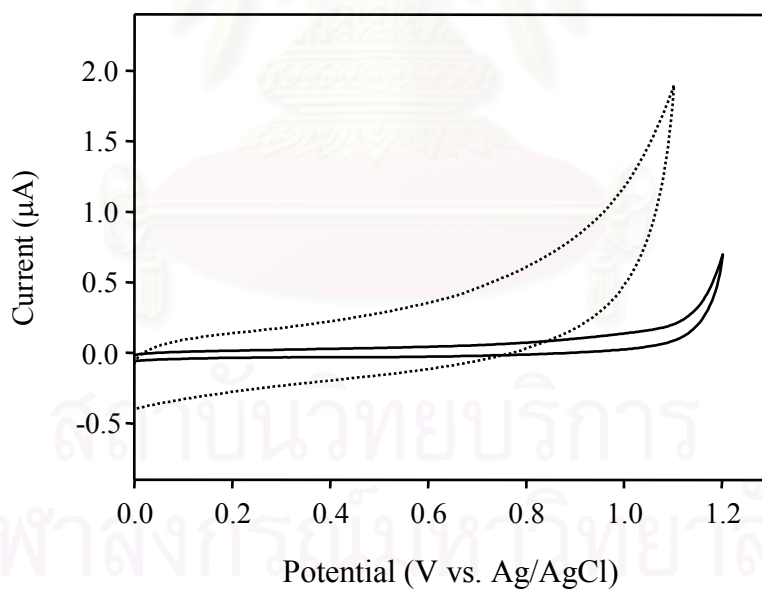


Figure 4.3 Cyclic voltammograms of 0.1 M phosphate buffer solution (pH 8) as the background at the BDD electrode (solid line) and the GC electrode (dash line). The scan rate was 50 mV s^{-1} . The area of electrode was 0.07 cm^2 .

4.1.3 The Scan Rate Dependence Study

The effect of the scan rate on the electrochemical behaviors of sulfite was studied by variation of the scan rate from 0.010 to 0.300 V s^{-1} . Cyclic voltammograms of sulfite at various scan rates are illustrated in Figure 4.4. The relationship between the peak current and the square root of the scan rate is shown in Figure 4.5. It was found that the peak current of sulfite was directly proportional to the square root of the scan rate. Thus it can be concluded that the diffusion process control the transportation of sulfite.

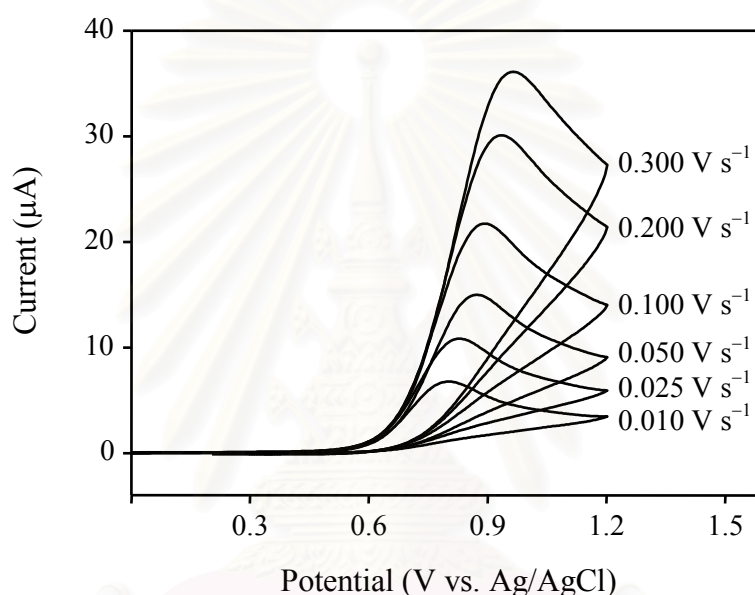


Figure 4.4 Cyclic voltammograms of 1 mM Na_2SO_3 in 0.1 M phosphate buffer solution (pH 8) at various scan rates for the BDD electrode. The area of electrode was 0.07 cm^2 .

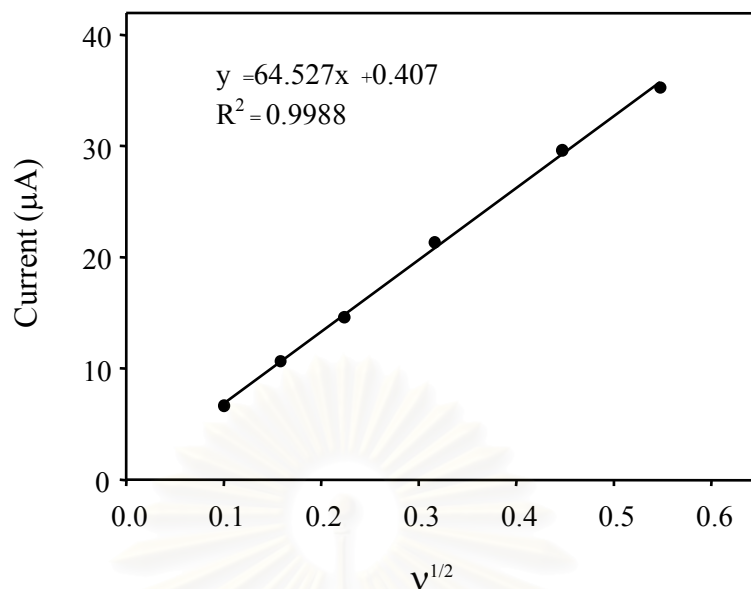


Figure 4.5 The relationship between the peak current and the square root of the scan rate ($v^{1/2}$).

4.2 Sequential Injection with Amperometric Detection

4.2.1 Optimum Potential for Amperometric Detection

Hydrodynamic voltammograms for the carrier (0.1 M phosphate buffer (pH 8)/0.1% SDS) and the 10 mg L^{-1} sulfite at various potential from 0.70 to 1.05 V are shown in Figure 4.6 and Figure 4.7 respectively. Peak currents and corresponding background currents obtained from hydrodynamic voltammograms were plotted as a function of applied potentials as illustrated in Figure 4.8. Each point of data for sulfite represented the average of peak currents for four consecutive injections. It was observed that the hydrodynamic voltammetric i -E curve did not provide a sigmoid shape. Thus S/B ratios were calculated and plotted as a function of potential as shown in Figure 4.9. The S/B ratio reached a maximum value at the potential of 0.95 V (versus Ag/AgCl). Therefore this potential was selected for amperometric detection in the next SIA experiment.

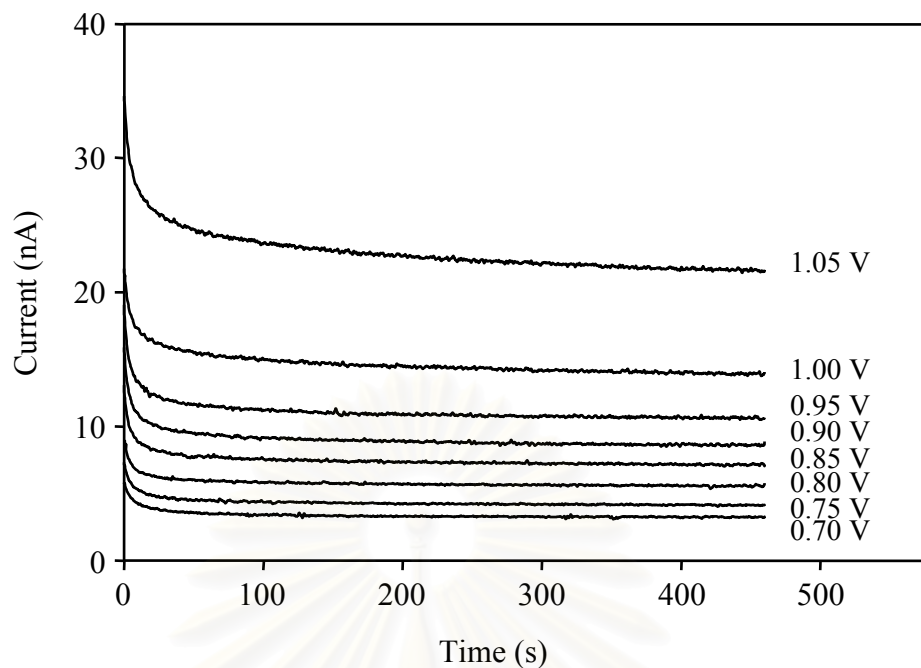


Figure 4.6 Hydrodynamic voltammograms for 0.1 M phosphate buffer (pH 8)/0.1% SDS (Background) at 0.70–1.05 V (vs. Ag/AgCl). The flow rate of carrier was 0.5 mL min⁻¹.

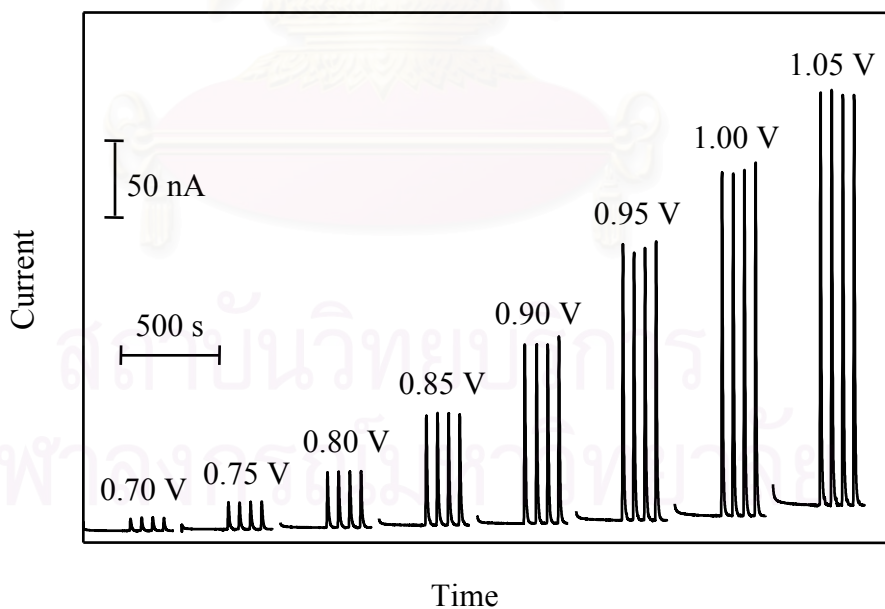


Figure 4.7 Hydrodynamic voltammogram for 10 mg L⁻¹ SO₃²⁻ (Signal) at 0.70–1.05 V (vs. Ag/AgCl). The SIA operating sequence was listed in Table 3.2. The flow rate of carrier was 0.5 mL min⁻¹.

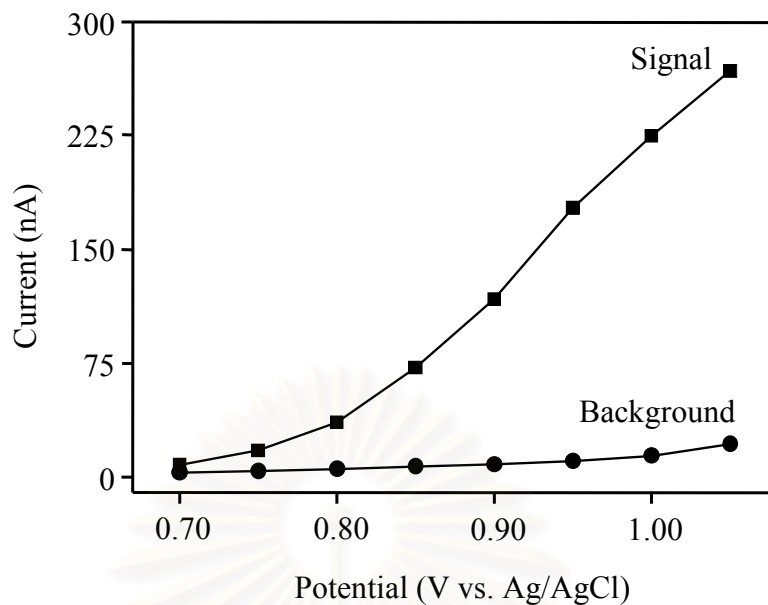


Figure 4.8 Hydrodynamic voltammetric i -E curve for $10 \text{ mg L}^{-1} \text{ SO}_3^{2-}$ (Signal) and 0.1 M phosphate buffer (pH 8)/ 0.1% SDS (Background).

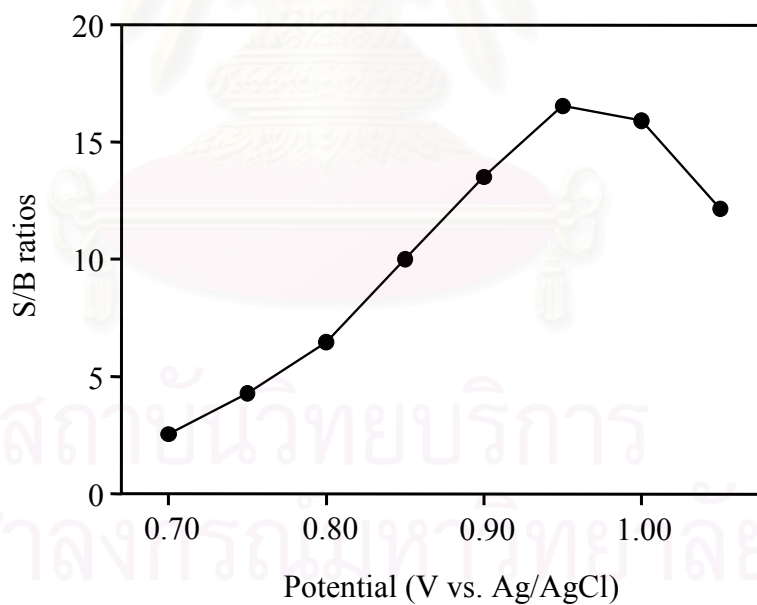


Figure 4.9 Relationship between potential and signal-to-background ratio.

4.2.2 Effect of Sodium Dodecyl Sulfate

The carrier solutions used in this SIA experiment were 0.1 M phosphate buffer (pH 8) and 0.1 M phosphate buffer (pH 8)/0.1% SDS. The peak currents obtained from fifteen consecutive injections of 10 mg L^{-1} sulfite for both carriers are shown in Figure 4.10. It was observed that after fifteen consecutive injections the peak current was reduced by about 30 % for the carrier solution of 0.1 M phosphate buffer (pH 8) while the peak current was still stable for the carrier solution of 0.1 M phosphate buffer (pH 8)/0.1% SDS. This result indicated that the 0.1% SDS can prevent the electrode fouling for the sulfite oxidation at the BDD electrode. For 0.001% SDS and 0.01% SDS, it was found that electrode fouling still occurred.

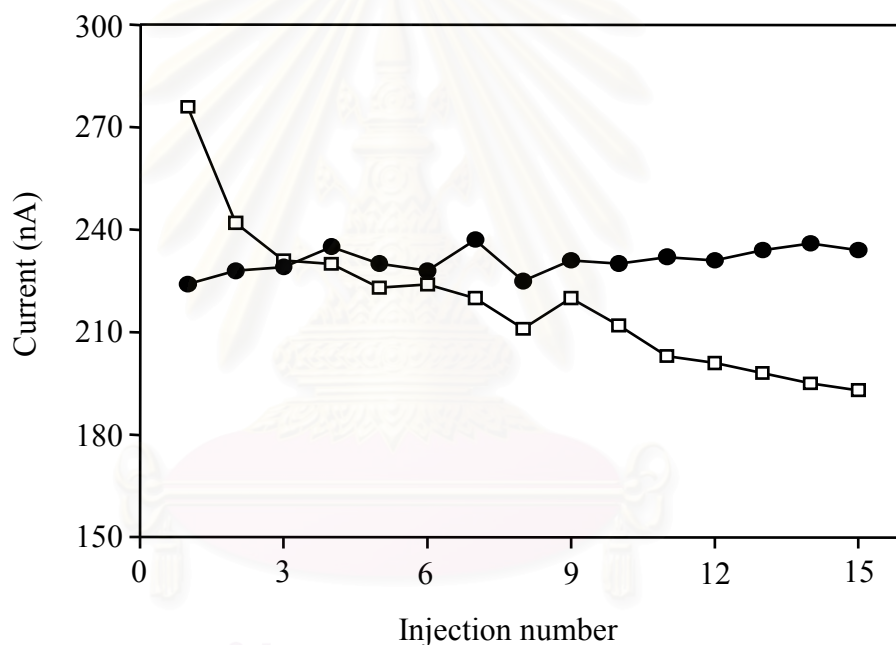


Figure 4.10 SIA with amperometric detection results for 15 consecutive injections of $10 \text{ mg L}^{-1} \text{ SO}_3^{2-}$. Carrier was 0.1 M phosphate buffer pH 8 (□) and 0.1 M phosphate buffer pH 8/0.1% SDS (●). The SIA operating sequence was listed in Table 3.2.

4.2.3 Sequential Injection Parameters

4.2.3.1 Sequence of Sulfite and Acid Aspiration

SIA with amperometric detection results obtained from four consecutive injections of sulfite (10 mg L^{-1} and 50 mg L^{-1}) for two SIA operating sequences are shown in Figure 4.11 and Figure 4.12. Sequence 1 represented the sulfite aspiration after the acid aspiration and Sequence 2 represented the acid aspiration after the sulfite aspiration. The average peak current and peak width are summarized in Table 4.2. From the result, the average peak currents of Sequence 1 are higher than those of Sequence 2, by about 39 % for 10 mg L^{-1} and 32 % for 50 mg L^{-1} . Therefore, the optimal sequence in the SIA experiment was the sulfite aspiration after the acid aspiration.

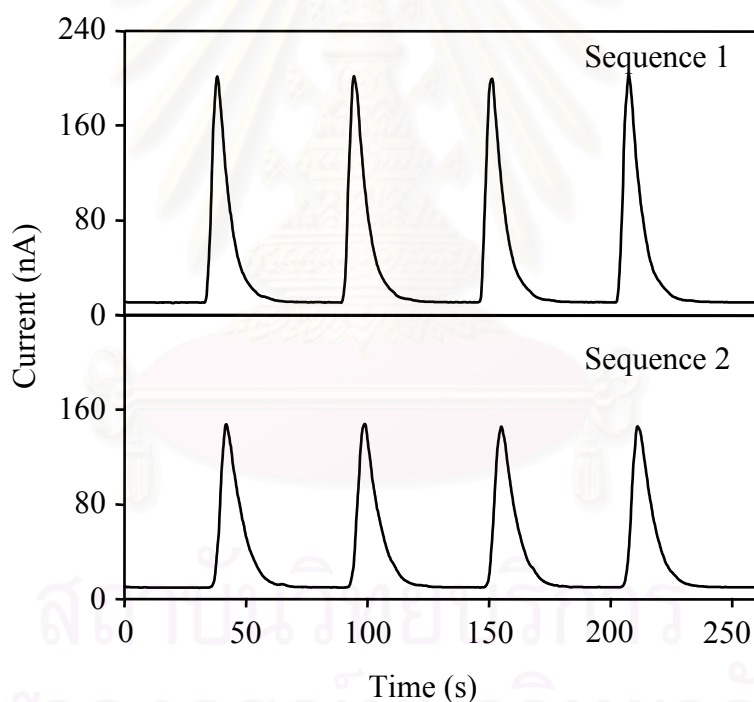


Figure 4.11 SIA with amperometric detection results of $10 \text{ mg L}^{-1} \text{ SO}_3^{2-}$ for two SIA operating sequences: Sequence 1, sulfite aspiration after acid aspiration; Sequence 2, acid aspiration after sulfite aspiration.

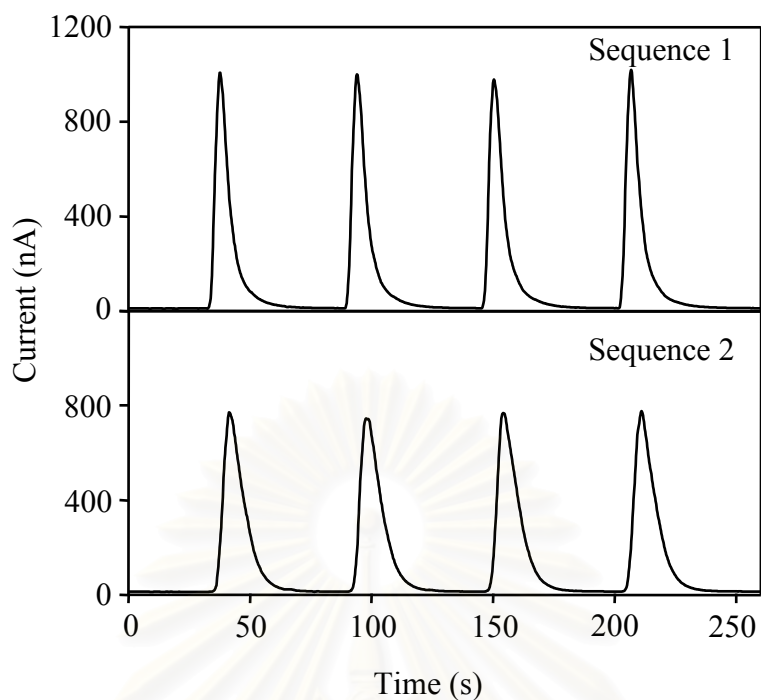


Figure 4.12 SIA with amperometric detection results of $50 \text{ mg L}^{-1} \text{ SO}_3^{2-}$ for two SIA operating sequences: Sequence 1, sulfite aspiration after acid aspiration; Sequence 2, acid aspiration after sulfite aspiration.

Table 4.2 Electrochemical data for two SIA operating sequences: Sequence 1, sulfite aspiration after acid aspiration; Sequence 2, acid aspiration after sulfite aspiration

Concentration of sulfite (mg L^{-1})	SIA sequence	Peak current (nA)	Peak width (s)
10	Sequence 1	190.7 ± 1.4	23.3 ± 0.6
	Sequence 2	136.9 ± 1.1	24.5 ± 0.8
50	Sequence 1	988.8 ± 17.1	24.6 ± 0.8
	Sequence 2	751.3 ± 13.7	24.5 ± 0.8

4.2.3.2 Volume of Sulfuric Acid

The volume of 2 M H₂SO₄ in the SIA operating sequence (step 2 in Table 3.2) was investigated over the range 20–140 μL. The average peak current and peak width for four consecutive injections of 10 mg L⁻¹ and 50 mg L⁻¹ sulfite are shown in Table 4.3 and Table 4.4 respectively. The relationship between the average peak current and the volume of 2 M H₂SO₄ is shown in Figure 4.13 for 10 mg L⁻¹ sulfite and Figure 4.14 for 50 mg L⁻¹ sulfite. It was observed that the peak current reached the plateau at the volume of 100 μL. Therefore, the volume of 100 μL was chosen as the optimum volume.

Aspiration of the second plug of 2 M H₂SO₄ (step 4 in Table 3.4) after sulfite aspiration was also studied over the range 0–60 μL. The average peak current and peak width for four consecutive injections of 10 mg L⁻¹ and 50 mg L⁻¹ sulfite are shown in Table 4.5 and Table 4.6, respectively. The relationship between the average peak current and the volume of 2 M H₂SO₄ is shown in Figure 4.15 for 10 mg L⁻¹ sulfite and Figure 4.16 for 50 mg L⁻¹ sulfite. It was observed that the peak current decreased as the volume of 2 M H₂SO₄ increased. The cause of this result is expected that there is the dispersion of generated sulfur dioxide in the second plug of 2 M H₂SO₄ on the other side of the sample zone. The dispersion of gaseous sulfur dioxide in 2 M H₂SO₄ is more than that in water because the form of sulfite in the acidic solution of 2 M H₂SO₄ is gaseous sulfur dioxide but forms of sulfite in water are HSO₃⁻ and SO₃²⁻ ions. Therefore, the aspiration of the second plug of acid on the other side of the sample decreased the sensitivity.

Table 4.3 The average peak current and peak width for 10 mg L⁻¹ sulfite at various volumes of 2 M H₂SO₄ in the SIA operating sequence (step 2 in Table 3.2)

Volume of 2 M H ₂ SO ₄ (μL)	Peak current (nA)	Peak width (s)
20	157.6 ± 4.3	23.4 ± 0.1
40	176.5 ± 2.9	23.7 ± 0.5
60	183.8 ± 3.3	23.9 ± 0.7
80	188.8 ± 1.8	24.5 ± 0.5
100	190.7 ± 1.4	24.2 ± 0.8
120	189.2 ± 1.7	23.5 ± 0.4
140	190.5 ± 1.3	24.8 ± 0.6

Table 4.4 The average peak current and peak width for 50 mg L⁻¹ sulfite at various volumes of 2 M H₂SO₄ in the SIA operating sequence (step 2 in Table 3.2)

Volume of 2 M H ₂ SO ₄ (μL)	Peak current (nA)	Peak width (s)
20	853.0 ± 10.6	25.2 ± 0.5
40	907.6 ± 17.6	24.7 ± 0.5
60	938.6 ± 7.1	24.7 ± 0.3
80	962.8 ± 23.2	26.9 ± 0.2
100	988.9 ± 17.1	26.1 ± 0.3
120	988.6 ± 17.9	27.0 ± 0.2
140	987.5 ± 15.9	27.1 ± 0.3

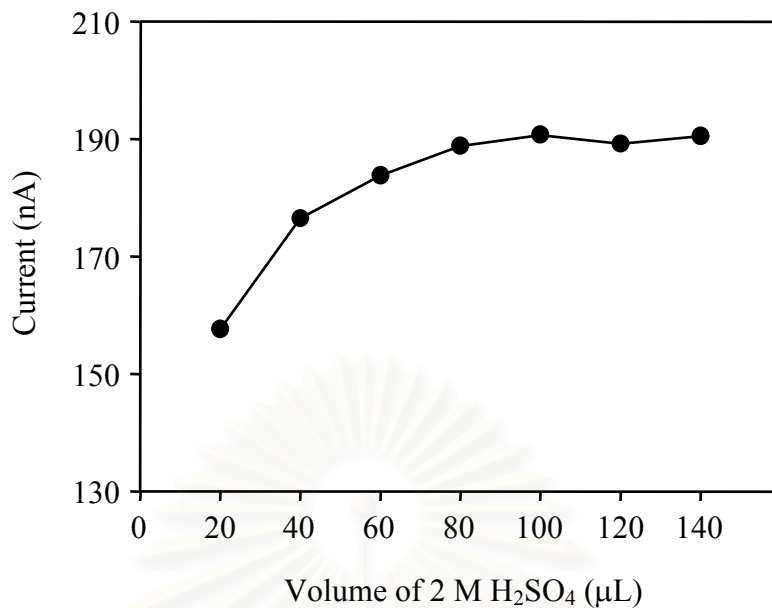


Figure 4.13 The relationship between the average peak current for 10 mg L⁻¹ sulfite and the volume of 2 M H₂SO₄ in the SIA operating sequence (step 2 in Table 3.2).

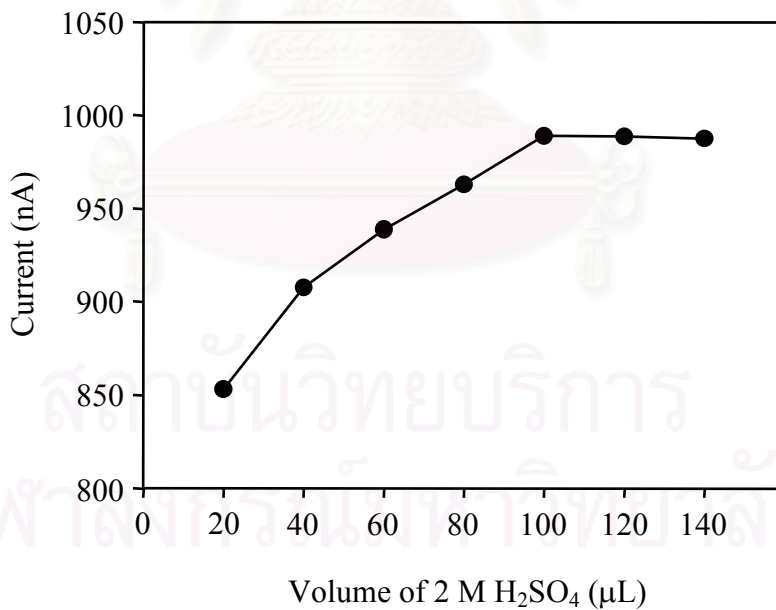


Figure 4.14 The relationship between the average peak current for 50 mg L⁻¹ sulfite and the volume of 2 M H₂SO₄ in the SIA operating sequence (step 2 in Table 3.2).

Table 4.5 The average peak current and peak width for 10 mg L⁻¹ sulfite at various volumes of 2 M H₂SO₄ in the SIA operating sequence (step 4 in Table 3.4)

Volume of 2 M H ₂ SO ₄ (μL)	Peak current (nA)	Peak width (s)
0	190.7 ± 1.4	23.3 ± 0.5
20	180.3 ± 2.2	25.8 ± 0.5
40	173.6 ± 2.2	24.9 ± 0.7
60	152.5 ± 3.5	25.3 ± 0.7

Table 4.6 The average peak current and peak width for 50 mg L⁻¹ sulfite at various volumes of 2 M H₂SO₄ in the SIA operating sequence (step 4 in Table 3.4)

Volume of 2 M H ₂ SO ₄ (μL)	Peak current (nA)	Peak width (s)
0	988.9 ± 17.1	25.6 ± 0.4
20	910.4 ± 9.1	24.4 ± 0.6
40	849.8 ± 14.4	23.7 ± 0.5
60	775.4 ± 10.7	24.5 ± 0.5

สถาบันวิทยบริการ
จุฬาลงกรณ์มหาวิทยาลัย

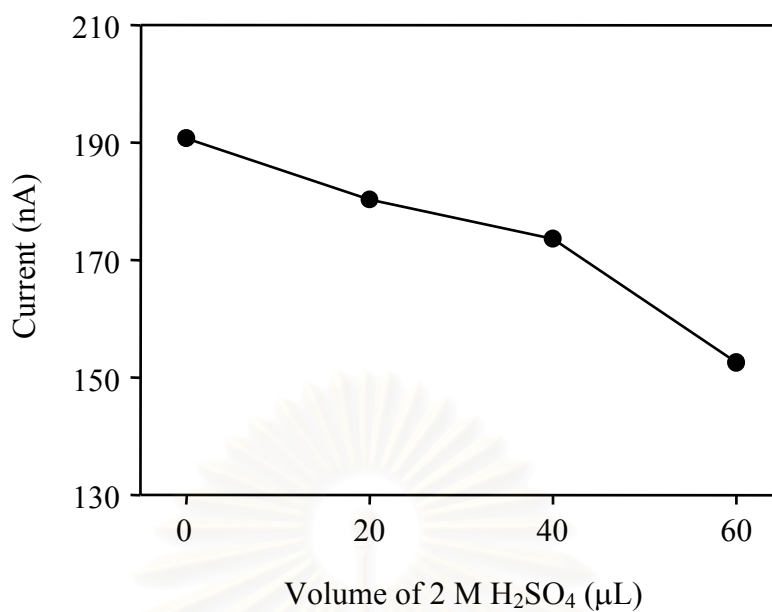


Figure 4.15 The relationship between the average peak current for 10 mg L⁻¹ sulfite and the volume of 2 M H₂SO₄ in the SIA operating sequence (step 4 in Table 3.4).

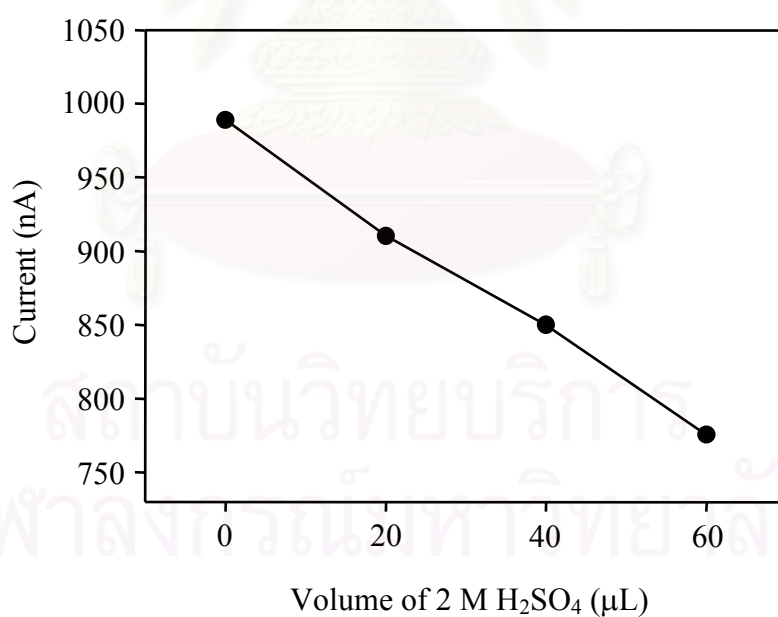


Figure 4.16 The relationship between the average peak current for 50 mg L⁻¹ sulfite and the volume of 2 M H₂SO₄ in the SIA operating sequence (step 4 in Table 3.4).

4.2.3.3 Propelling Flow Rate

The flow rate for propelling the acidified sample to the donor channel of the GDU was investigated over the range 10–35 $\mu\text{L s}^{-1}$. SIA with amperometric detection results for four consecutive injections of 10 mg L^{-1} sulfite at various flow rates are shown in Figure 4.17. The average peak current and peak width are shown in Table 4.7. From Figure 4.17 it was observed that the time of analysis decreased as the flow rate increased. As shown in Table 4.7 the highest peak current was obtained at the flow rate of 25 $\mu\text{L s}^{-1}$. Thus, the flow rate of 25 $\mu\text{L s}^{-1}$ was selected for the SIA experiment.



สถาบันวิทยบริการ
จุฬาลงกรณ์มหาวิทยาลัย

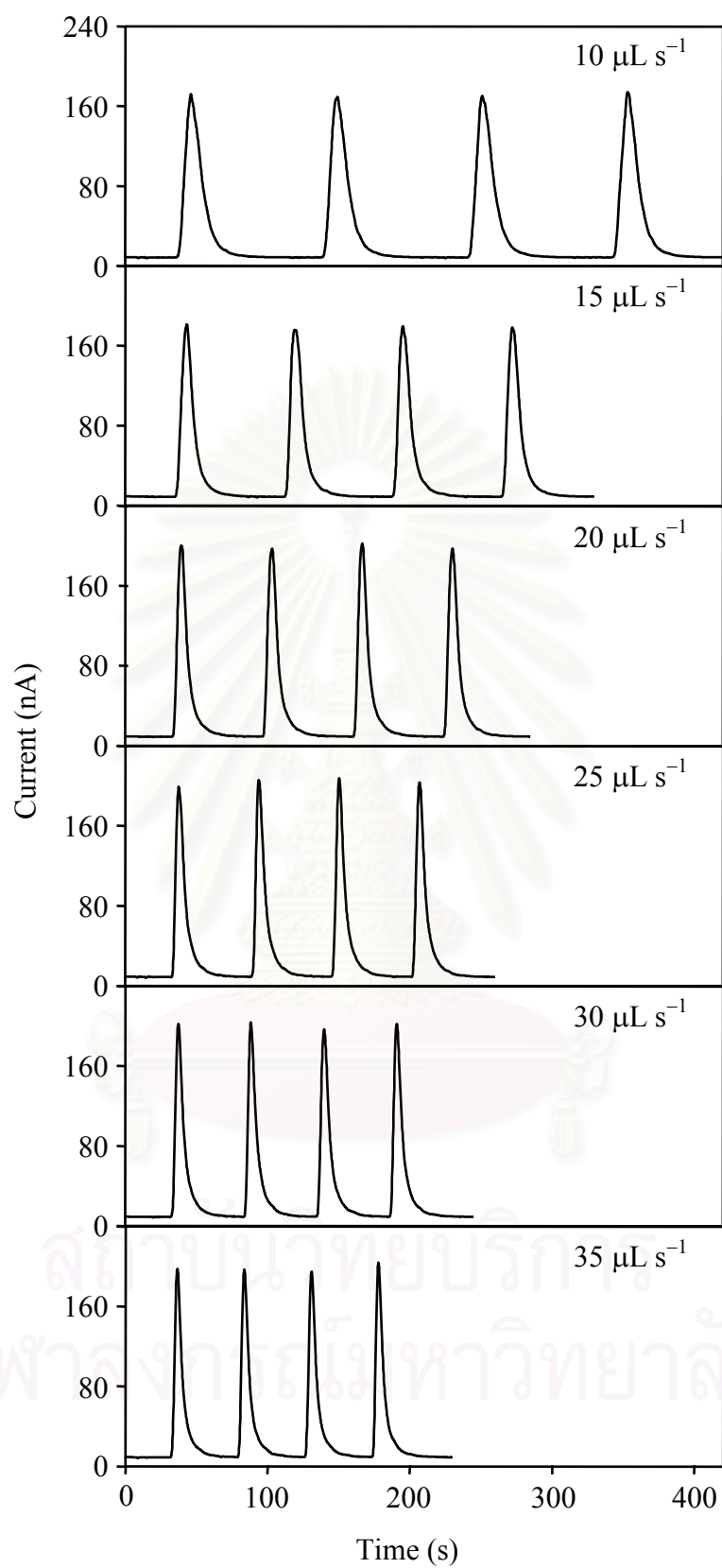


Figure 4.17 SIA with amperometric detection results for 10 mg L^{-1} sulfite at various flow rates for propelling the acidified sample to the GDU.

Table 4.7 The average peak current and peak width for 10 mg L⁻¹ sulfite at various flow rates for propelling the acidified sample to the GDU

Flow rate ($\mu\text{L s}^{-1}$)	Peak current (nA)	Peak width (s)
10	162.7 ± 2.1	32.0 ± 0.2
15	170.0 ± 2.3	30.1 ± 0.6
20	190.1 ± 2.5	26.1 ± 0.5
25	194.9 ± 3.6	25.0 ± 0.6
30	191.8 ± 3.0	24.4 ± 0.5
35	189.1 ± 3.8	23.0 ± 0.5

4.2.3.4 Flow Rate of Carrier

The flow rate of carrier for carrying sulfite to the electrochemical flow cell was studied over the range 0.25–1.0 mL min⁻¹ at intervals of 0.25 mL min⁻¹. SIA with amperometric detection results for four consecutive injections of 10 mg L⁻¹ sulfite at various flow rates are shown in Figure 4.18. The average peak current and peak width are shown in Table 4.8. It was observed that the signal current increased as the flow rate of carrier decreased. However, the peak width at the flow rate of 0.25 mL min⁻¹ is much broader than that at the flow rate of 0.5 mL min⁻¹. This result can be explained that the content of gaseous sulfur dioxide, which diffused through the membrane into the carrier, increased as the flow rate decreased but sample dispersion in the carrier also increased. Therefore the flow rate of 0.5 mL min⁻¹ was the chosen value as a compromise between sensitivity and sampling frequency.

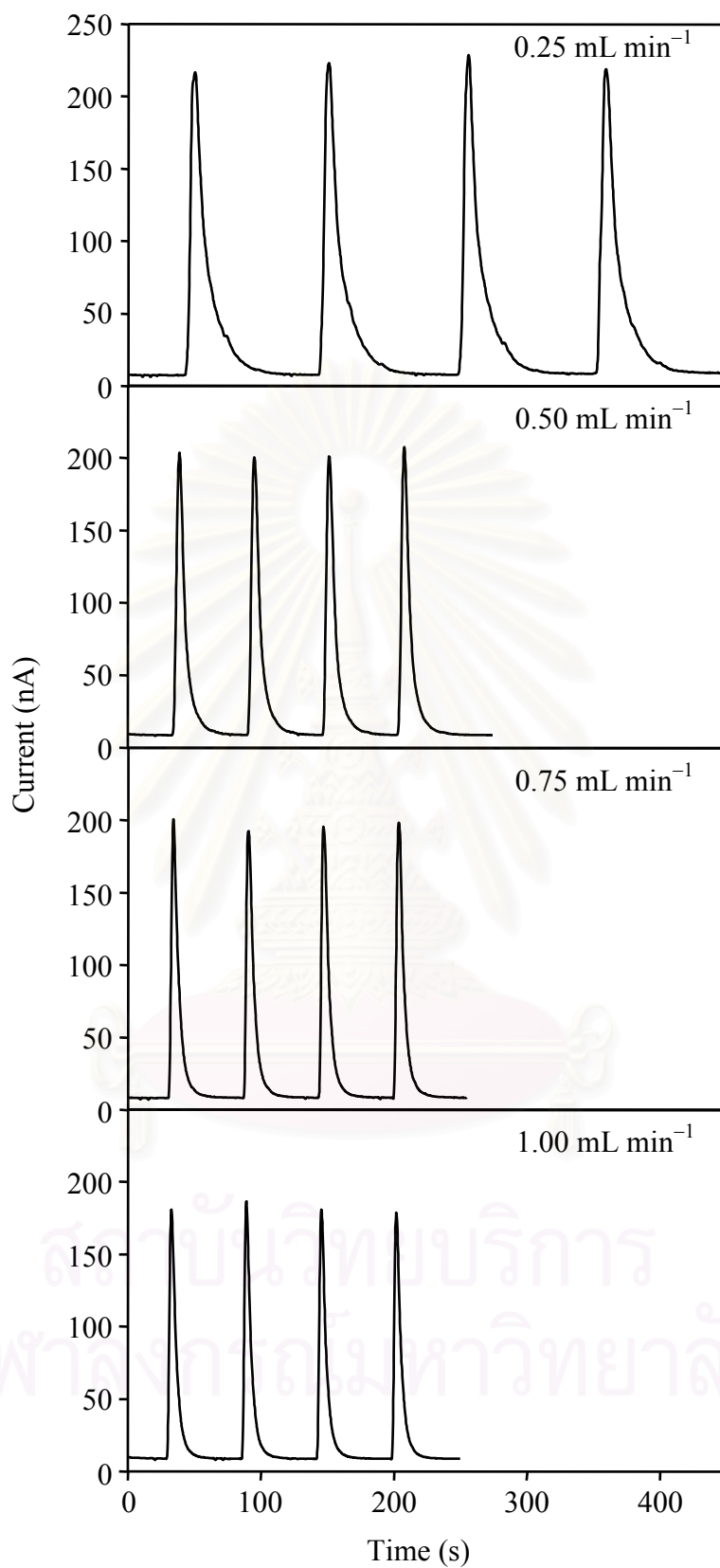


Figure 4.18 SIA with amperometric detection results for 10 mg L⁻¹ sulfite at various flow rates of carrier.

Table 4.8 The average peak current and peak width for 10 mg L⁻¹ sulfite at various flow rates of carrier

Flow rate (mL min ⁻¹)	Peak current (nA)	Peak width (s)
0.25	213.7 ± 5.2	42.3 ± 0.8
0.50	194.4 ± 3.2	25.2 ± 0.2
0.75	188.5 ± 3.6	18.7 ± 0.4
1.00	173.0 ± 3.3	16.4 ± 0.4

4.2.4 Influence of Sample Volume

The sample volume in the SIA operating sequence (step 3 in Table 3.2) was studied over the range 10–50 µL at intervals of 10 µL. The average peak current and peak width for four consecutive injections of 10 mg L⁻¹ sulfite at various volumes are shown in Figure 4.19. The relationship between the average peak current and the sample volume is shown in Figure 4.9. From these results, signal currents increase with increasing sample volume. For example, signal currents increase about six times when sample volume was increased from 10 µL to 50 µL. This result indicated that the linear range of the SIA method can be changed easily by changing sample volume aspirated into holding. This is an interested choice of the SIA method for the gas diffusion separation in addition to the reduction of both reagent consumption and volume of effluent. The sample containing the high content of sulfite can be analyzed by reducing the sample volume in the SIA operating sequence without dilution. For wine, any change in composition of the wine, like dilution, will inevitably shift the equilibrium between bound and free sulfite [39].

Table 4.9 The average peak current and peak width for 10 mg L^{-1} sulfite at various sample volumes

Sample volume (μL)	Peak current (nA)	Peak width (s)
10	30.0 ± 0.2	20.1 ± 0.8
20	68.6 ± 1.0	21.9 ± 0.4
30	109.0 ± 1.9	22.2 ± 0.3
40	145.1 ± 2.4	23.0 ± 0.5
50	176.0 ± 2.7	23.0 ± 0.4

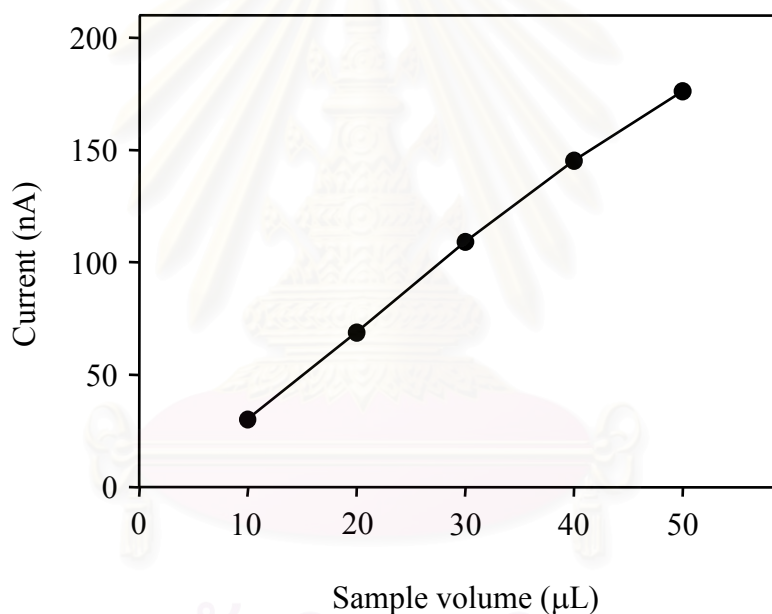


Figure 4.19 The relationship between the average peak current and the sample volume for 10 mg L^{-1} sulfite.

4.2.5 Linearity

The concentration of sulfite was studied over the range $0.2\text{--}50 \text{ mg L}^{-1}$ to find the linearity. The average peak current and peak width for four consecutive injections of sulfite at various concentrations are shown in Table 4.10. The linear dynamic range and linear regression equation illustrated in Figure 4.20 were obtained by the least square method. A linear dynamic range of $0.2\text{--}20 \mu\text{L mg L}^{-1}$ for sulfite was obtained with a correlation coefficient of 0.9997.

Table 4.10 The average peak current and peak width for various concentrations of sulfite

Concentration of sulfite (μL)	Peak current (nA)	Peak width (s)
0.2	3.3 ± 0.2	19.1 ± 0.5
0.5	9.7 ± 0.3	20.9 ± 0.6
1.0	21.2 ± 0.4	22.0 ± 0.7
2.5	54.1 ± 0.9	24.0 ± 0.8
5.0	106.4 ± 1.5	23.4 ± 0.3
10	205.7 ± 2.1	24.0 ± 0.7
15	313.2 ± 4.0	24.6 ± 0.8
20	406.9 ± 2.2	24.2 ± 0.5
30	576.2 ± 7.7	23.6 ± 0.4
40	750.1 ± 7.2	24.5 ± 0.3
50	905.0 ± 17.4	24.2 ± 0.3

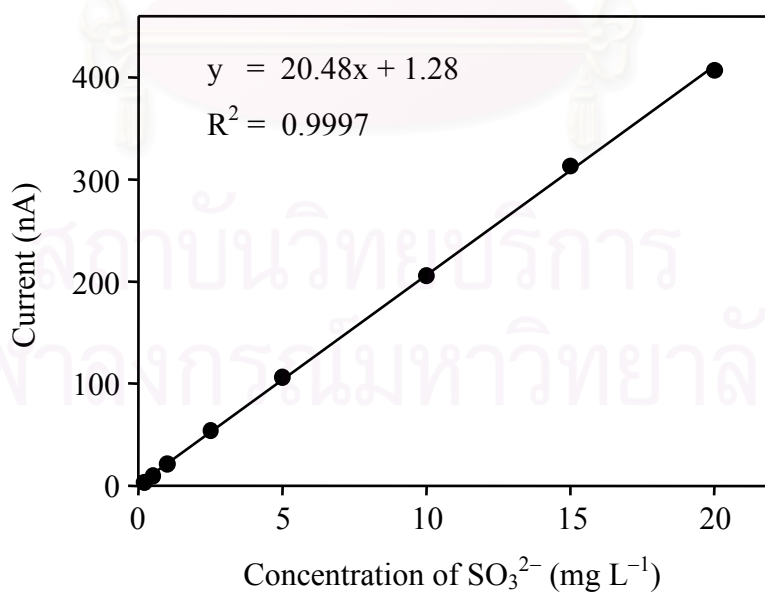


Figure 4.20 Calibration curve of sulfite.

4.2.6 Limit of Detection

The concentration of sulfite was studied over the range 0–0.2 mg L⁻¹ to obtain the limit of detection. The limit of detection, based on a signal-to-noise ratio (S/N) of 3, was found to be 0.05 mg L⁻¹ SO₃²⁻. SIA with amperometric detection results for four consecutive injections of blank and 0.05 mg L⁻¹ sulfite are shown in Figure 4.21.

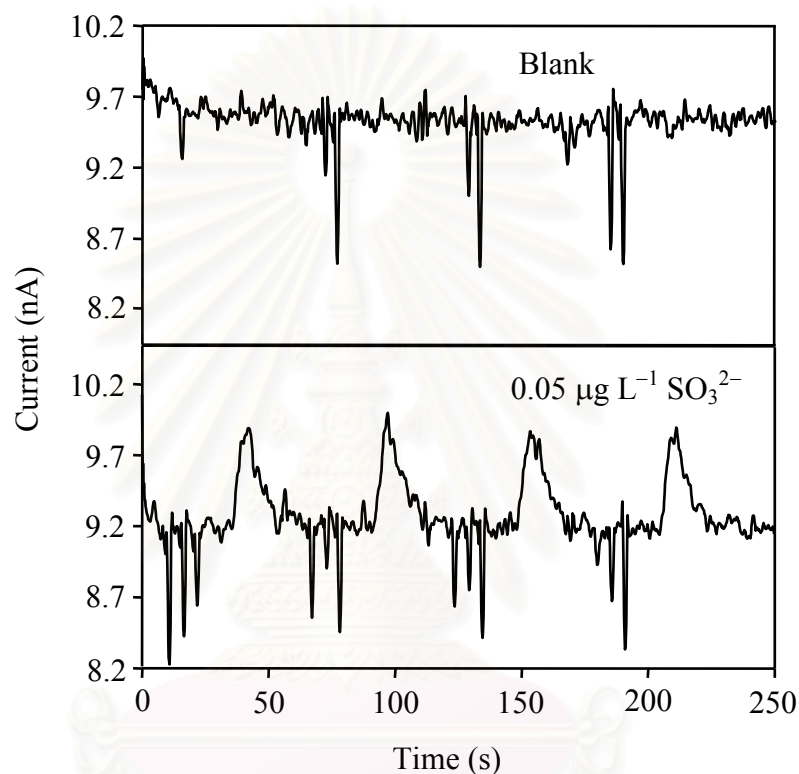


Figure 4.21 SIA with amperometric detection results for blank and 0.05 mg L⁻¹ sulfite.

สถาบันวิทยบริการ
จุฬาลงกรณ์มหาวิทยาลัย

4.2.7 Repeatability

SIA with amperometric detection results for ten consecutive injections of 10 mg L^{-1} sulfite are shown in Figure 4.22. The relative standard deviation of the proposed SI system was found to be 1.38 %.

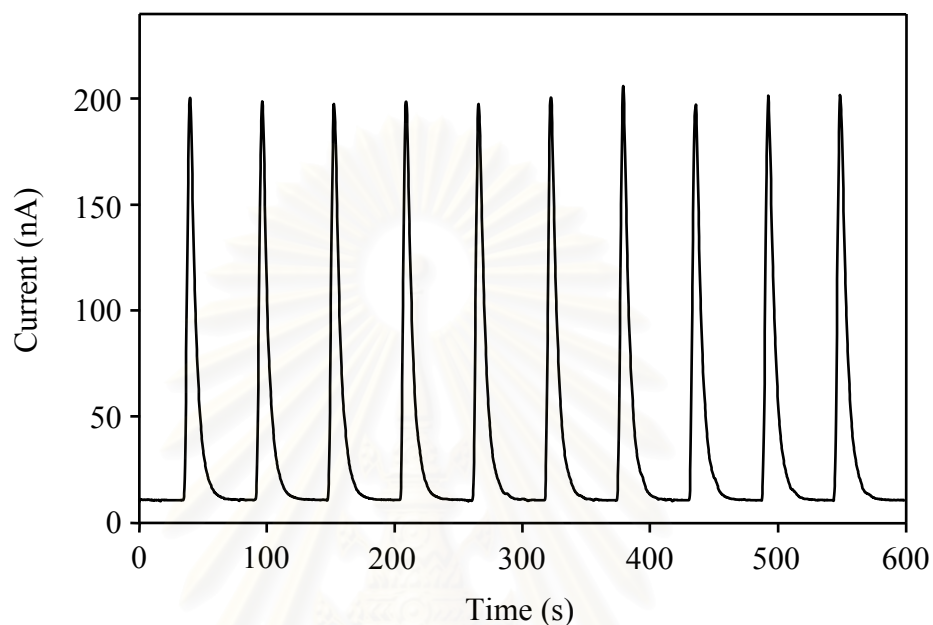


Figure 4.22 SIA with amperometric detection results for ten consecutive injections of 10 mg L^{-1} sulfite.

4.3 Real sample analysis

4.3.1 Effect of Ethanol

The effect of ethanol in sulfite solution on the signal current was investigated by varying the concentration of ethanol over the range 0–14 % (v/v). From the SIA with amperometric detection results for four consecutive injections, the average peak current was obtained. The relationship between the peak current and the percentage of ethanol is illustrated in Figure 4.23. It was observed that the peak current reached the plateau at the 6 % of ethanol. It was also observed that the peak current increase about 36 % as the concentration of ethanol increase from 0 to 6 %. The cause of this result is expected that the composition of the carrier changes because the ethanol can diffuse through the membrane into the carrier. Sullivan [50] reported the stabilizing effect of ethanol when it was added to standard solutions of sulfite. Therefore, the current signal of sulfite is increased. Decnop-Weever et al. [39] reported that addition of 10% ethanol to the donor and acceptor solutions is crucial to obtain reliable results. In this work, 10 % of ethanol was added in the standard solution of sulfite for matrix matching.

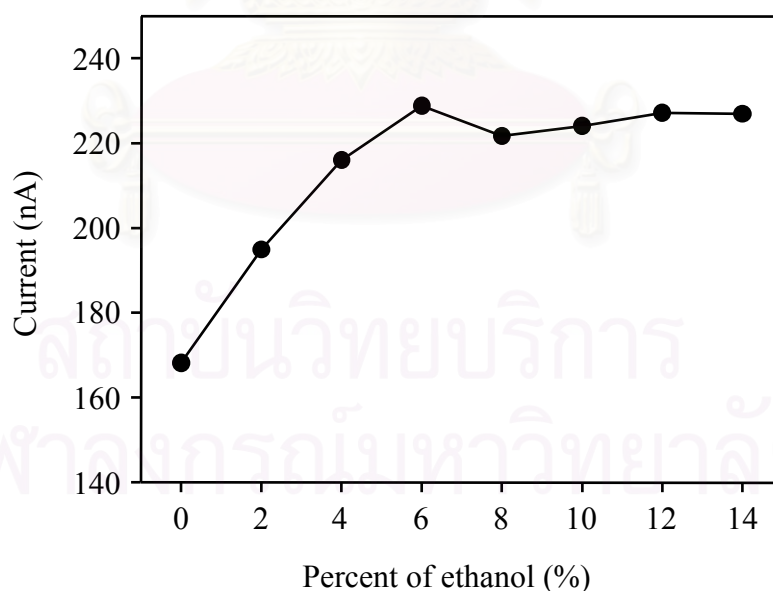


Figure 4.23 The relationship between the average peak current for 10 mg L⁻¹ sulfite and the percent of ethanol in sulfite solution.

4.3.2 Determination of Sulfur Dioxide in Wines

In order to evaluate the accuracy of the proposed system, the method was applied to the determination of free and total sulfur dioxide in wines. The analytical results were compared with those obtained by iodimetric titration. The results obtained by both methods are shown in Table 2. The experimental *t*-values obtained by the proposed SIA method were 0.532 for free sulfur dioxide and 0.914 for total sulfur dioxide. These *t*-values were smaller than the *t*-value (3.182) for three degrees of freedom at the 95% confidence level. This indicates that there is no significant difference between the results obtained by the proposed SIA method and those of the iodimetric titrations. The relative standard deviations for the analysis of sulfite in wines were in the range of 1.0 – 4.1 %.

Table 4.11 Comparison of the results obtained by SIA and titration methods for free and total SO₂ in wines

Sample	Free SO ₂ (mg L ⁻¹) ^a		Total SO ₂ (mg L ⁻¹) ^a	
	SIA method	Titration method	SIA method	Titration method
White wine 1	11.2 ± 0.3	11.9 ± 0.4	48.7 ± 0.9	47.5 ± 1.9
White wine 2	24.1 ± 0.3	22.2 ± 0.4	102.4 ± 1.1	105.8 ± 0.9
Red wine 1	11.9 ± 0.2	11.7 ± 0.4	55.2 ± 0.8	58.3 ± 0.9
Red wine 2	5.1 ± 0.1	5.3 ± 0.4	32.6 ± 1.3	31.8 ± 1.6

^a Mean ± standard deviation (n=3)

Because the iodimetric titration is not the standard method for the determination of sulfur dioxide in wine, thus comparison between the proposed SIA method and the standard method is better. In the AOAC Official Method, sulfur dioxide in wine is determined by flow injection analysis using reaction with malachite green. For the determination of free sulfur dioxide [51], test solution is acidified to produce SO₂ gas, which diffuses across Teflon membrane in gas diffusion cell into flowing stream of malachite green, which is discolored. Degree of discoloration of malachite green which is proportional to amount of sulfite in test solution is measured spectrophotometrically. For the determination of total sulfur dioxide [52], test solution is first reacted with NaOH to liberate bound sulfite. Then test stream is acidified to

produce SO₂ gas, which diffuses across Teflon membrane in gas diffusion cell into flowing stream of malachite green. Degree of discoloration of malachite green is measured spectrophotometrically. In this work, these AOAC Official methods can not be performed because the spectrophotometric detector for FIA is unavailable. Thus the iodimetric titration was used for comparison.

4.4 Comparison of the proposed SIA method with Other Methods

Analytical characteristics of the proposed SIA and some flow-based methods for sulfite analysis were summarized in Table 4.12 for comparison. It was found that the proposed method provided wider linear range and higher sensitivity, compared with other flow-based method. The proposed SIA method also provided high sample throughput and low reagent consumption. The sampling frequency was 65 determinations per hour. The consumption of 2 M H₂SO₄ per determination was 100 µL and the volume of 0.1 M phosphate buffer (pH 8)/0.1% SDS per determination was about 0.5 mL.

Table 4.12 Comparison of analytical characteristics of the proposed SIA and some flow-based methods

Method for sulfite analysis	Linear range (mg L ⁻¹ SO ₃ ²⁻)	Detection limit (mg L ⁻¹ SO ₃ ²⁻)	RSD (%)	Sampling rate (h ⁻¹)	Reference
Proposed SIA method (GD–SIA with amperometric detection using BDD electrode)	0.2–20	0.05	1.4	65	–
FIA with amperometric detection using a poly[Ni-(protoporphyrin IX)] modified electrode	up to 11	0.2	<6.9	–	[44]
GD–FIA with amperometric detection using Pt electrode	0.3–20	0.06	4	30	[40]
GD–FIA with spectrophotometric detection using bromocresol green for pH detection	1–20	0.1	<1.5 %	120	[39]
GD–SIA with spectrophotometric detection using pararosaniline	2.5–50 ^(a) 30–300 ^(b)	0.1 ^(a) 0.7 ^(b)	<1.2 ^(a) <2.3 ^(b)	16	[18]

^(a) Analytical characteristics for free SO₂

^(b) Analytical characteristics for total SO₂

CHAPTER V

CONCLUSIONS

5.1 Conclusions

A boron-doped diamond (BDD) electrode has advantages over the glassy carbon (GC) electrode for the detection of sulfite. The BDD electrode provided higher signal. Especially the background current obtained from the BDD electrode was about eight times smaller than that obtained from the GC electrode. Thus higher sensitivity was obtained for the BDD electrode, compared to the GC electrode.

The use of a gas diffusion-sequential injection system with the BDD electrode for sulfite determination proved to be an effective alternative. The addition of 0.1% sodium dodecyl sulfate into the carrier of 0.1 M phosphate buffer (pH 8) can prevent electrode fouling. The SIA manifold for sulfite analysis is simple. Under the optimum condition, the linear range over two orders of magnitude was 0.2–20 mg L⁻¹ and the detection limit of 0.05 mg L⁻¹ for sulfite was achieved. The sensitivity of the presented method is better than that of the other flow-based methods as shown in Table 4.12. The sensitivity of the method can be changed easily by changing the sample volume which is an advantage of the SIA over the FIA. Other advantages of the presented system are the use of few and non-toxic reagents and the reduction of both reagent consumption and volume of effluent. Solutions of 2 M sulfuric acid and 0.1 M phosphate buffer (pH 8)/0.1% SDS were used only. The consumption of 2 M sulfuric acid and 0.1 M phosphate buffer (pH 8)/0.1% SDS per determination were 100 µL and 0.5 mL respectively. The presented method provided high sample throughput. The sampling frequency was 65 determinations per hour.

The developed SIA system allowed the determination of free and total sulfur dioxide in different types of wines. The sample containing high content of sulfur dioxide was analyzed by reducing the sample volume in the SIA operating sequence from 50 µL to 15 µL. There is no significant difference between the results obtained by the proposed method and the iodimetric titration. The relative standard deviations for the analysis of sulfur dioxide in wines were in the range of 1.0–4.1 %. Application of the proposed method for the determination of sulfur dioxide in wines shows that this method is accurate and precise.

1.2 Suggestion for Further Work

In this study, the real samples studied were only wine samples. Other samples such as dried longan or rice vermicelli should be of particular interest for this study as well. Also the proposed method can be applied to other analytes, such as iodide, mercury and arsenic. These analytes react with some reagents and generate gases or substances which can diffuse through the membrane into the proper acceptor solution. The electroactive species were then generated and detected at the BDD electrode.

Improving the sensitivity of the proposed system is another interesting aspect. The sensitivity can be improved by using the syringe pump instead of the peristaltic pump for the carrier. The pump is set to operate only after all donor solution flow through the donor channel of the GDU. This result in the accumulation of the analyte in the acceptor channel of the GDU, thus the sensitivity is increased.



REFERENCES

- [1] Sawyer, D. T.; Sobkowiak, A.; and Roberts, J. L. Electrochemistry for Chemists. 2nded. New York: Wiley Interscience, 1995.
- [2] Settle, F. A. Handbook of Instrumental Techniques for Analytical Chemistry. New Jersey: Prentice Hall, 1997.
- [3] Thomas, F. G.; and Henze, G. Introduction to Voltammetric Analysis. Collingwood, Australia: CSIRO Publishing, 2001.
- [4] Skoog, D. A.; West, D. M.; Holler, F. J.; and Crouch, S. R. Fundamentals of Analytical Chemistry. 8thed. London: Thomson Brooks/Cole, 2004.
- [5] Buchberger, W. W. Detection techniques in ion analysis: what are our choices? J. Chromatogr. A 884 (2000): 3-22.
- [6] Trojanowicz, M. Flow Injection Analysis: Instrumentation and Applications. Singapore: World Scientific, 2000.
- [7] Xu, J. S.; Granger, M. C.; Chen, Q. Y.; Strojek, J. W.; Lister, T. E.; and Swain, G. M. Boron-doped diamond thin-film electrodes. Anal. Chem. 69 (1997): A591-A597.
- [8] Rao, T. N.; Fujishima, A.; Angus, J. C.; Yasuaki, E.; and Tryk, D. A. Diamond Electrochemistry. Amsterdam: Elsevier Science, 2005.
- [9] Kraft, A. Doped Diamond: A Compact Review on a New, Versatile Electrode Material. Int. J. Electrochem. Sci. 2 (2007): 355-385.
- [10] Economou, A. Sequential-injection analysis (SIA): A useful tool for on-line sample-handling and pre-treatment. TrAC, Trends Anal. Chem. 24 (2005): 416-425.
- [11] Ruzicka, J.; and Hansen, E. H. Flow injection analyses: Part I. A new concept of fast continuous flow analysis. Anal. Chim. Acta 78 (1975): 145-157.
- [12] Stewart, K. K.; Beecher, G. R.; and Hare, P. E. Rapid analysis of discrete samples: The use of nonsegmented, continuous flow. Anal. Biochem. 70 (1976): 167-173.
- [13] Perez-Olmos, R.; Soto, J. C.; Zarate, N.; Araujo, A. N.; and Montenegro, M. C. B. S. M. Sequential injection analysis using electrochemical detection: A review. Anal. Chim. Acta 554 (2005): 1-16.

- [14] Barnett, N. W.; Lenehan, C. E.; and Lewis, S. W. Sequential injection analysis: an alternative approach to process analytical chemistry. TrAC, Trends Anal. Chem. 18 (1999): 346-353.
- [15] Ruzicka, J.; and Marshall, G. D. Sequential injection: a new concept for chemical sensors, process analysis and laboratory assays. Anal. Chim. Acta 237 (1990): 329-343.
- [16] Marshall, G.; Wolcott, D.; and Olson, D. Zone fluidics in flow analysis: potentialities and applications. Anal. Chim. Acta 499 (2003): 29-40.
- [17] Kuban, P.; and Karlberg, B. Interfacing of flow injection pre-treatment systems with capillary electrophoresis. TrAC, Trends Anal. Chem. 17 (1998): 34-41.
- [18] Segundo, M. A.; and Rangel, A. O. S. S. A gas diffusion sequential injection system for the determination of sulphur dioxide in wines. Anal. Chim. Acta 427 (2001): 279-286.
- [19] Mesquita, R. B. R.; and Rangel, A. O. S. S. Gas diffusion sequential injection system for the spectrophotometric determination of free chlorine with o-dianisidine. Talanta 68 (2005): 268-273.
- [20] Oms, M. T.; Cerda, A.; Cladera, A.; Cerda, V.; and Forteza, R. Gas diffusion techniques coupled sequential injection analysis for selective determination of ammonium. Anal. Chim. Acta 318 (1996): 251-260.
- [21] Branen, A. L.; Davidson, M. P.; Salminen, S.; and Thorngate III, H. J. Food additives. New York: Marcel Dekker, Inc., 2002.
- [22] Davidson, P. M.; Sofos, J. N.; and Branen, A. L. Antimicrobials in Food. 3rded. New York: Taylor & Francis, 2005.
- [23] King, A. D.; Ponting, J. D.; Sanshuk, D. W.; Jackson, R.; and Mihara, K. Factors affecting death of yeast by sulfur dioxide. J. Food Prot. 44 (1981): 92-97.
- [24] Rehm, H. J.; and Wittmann, H. Beitrag zur Kenntnis der antimikrobiellen Wirkung der schwefligen Säure. Z. Lebensm. Unters. Forsch. 118 (1962): 413-429.
- [25] Lund, B. M.; Baird-Parker, T. C.; and Gould, G. W. The Microbiological Safety and Quality of Food. Maryland: Aspen Publishers, 2000.
- [26] Jackson, R. S. Wine Science: Principles, Practice, Perception. 2nded. California: Academic Press, 2000.
- [27] Official Method 990.28 Official Methods of Analysis of AOAC International. Maryland: AOAC International, 2000.

- [28] Li, Y.; and Zhao, M. Simple methods for rapid determination of sulfite in food products. Food Control 17 (2006): 975-980.
- [29] Zhan, X. Q.; Li, D. H.; Zheng, H.; and Xu, J. G. Fluorimetric determination of sulfite by the co-quenching effect of formaldehyde and sulfite on the fluorescence of tetra-substituted amino aluminum phthalocyanine. Anal. Chim. Acta 448 (2001): 71-77.
- [30] Yang, X. F.; Guo, X. Q.; and Zhao, Y. B. Novel spectrofluorimetric method for the determination of sulfite with rhodamine B hydrazide in a micellar medium. Anal. Chim. Acta 456 (2002): 121-128.
- [31] Meng, H.; Wu, F.; He, Z.; and Zeng, Y. Chemiluminescence determination of sulfite in sugar and sulfur dioxide in air using Tris(2,2'-bipyridyl)ruthenium(II)-permanganate system. Talanta 48 (1999): 571-577.
- [32] Pournaghi-Azar, M. H.; Hydarpour, M.; and Dastango, H. Voltammetric and amperometric determination of sulfite using an aluminum electrode modified by nickel pentacyanonitrosylferrate film: Application to the analysis of some real samples. Anal. Chim. Acta 497 (2003): 133-141.
- [33] Garcia, T.; Casero, E.; Lorenzo, E.; and Pariente, F. Electrochemical sensor for sulfite determination based on iron hexacyanoferrate film modified electrodes. Sens. Actuators, B 106 (2005): 803-809.
- [34] Casella, I. G.; and Marchese, R. Sulfite oxidation at a platinum glassy carbon electrode. Determination of sulfite by ion exclusion chromatography with amperometric detection. Anal. Chim. Acta 311 (1995): 199-210.
- [35] Pizzoferrato, L.; Di Lullo, G.; and Quattrucci, E. Determination of free, bound and total sulphites in foods by indirect photometry-HPLC. Food Chem. 63 (1998): 275-279.
- [36] Trenerry, V. C. The determination of the sulphite content of some foods and beverages by capillary electrophoresis. Food Chem. 55 (1996): 299-303.
- [37] Jankovskiene, G.; Daunoravicius, Z.; and Padarauskas, A. Capillary electrophoretic determination of sulfite using the zone-passing technique of in-capillary derivatization. J. Chromatogr. A 934 (2001): 67-73.
- [38] Lin, J. M.; and Hobo, T. Flow-injection analysis with chemiluminescent detection of sulphite using Na_2CO_3 --- NaHCO_3 - Cu^{2+} system. Anal. Chim. Acta 323 (1996): 69-74.

- [39] Decnop-Weever, L. G.; and Kraak, J. C. Determination of sulphite in wines by gas-diffusion flow injection analysis utilizing spectrophotometric pH-detection. Anal. Chim. Acta 337 (1997): 125-131.
- [40] Cardwell, T. J.; and Christophersen, M. J. Determination of sulfur dioxide and ascorbic acid in beverages using a dual channel flow injection electrochemical detection system. Anal. Chim. Acta 416 (2000): 105-110.
- [41] Mana, H.; and Spohn, U. Sensitive and selective flow injection analysis of hydrogen sulfite/sulfur dioxide by fluorescence detection with and without membrane separation by gas diffusion. Anal. Chem. 73 (2001): 3187-3192.
- [42] Bonifacio, R. L.; and Coichev, N. Chemiluminescent determination of sulfite traces based on the induced oxidation of Ni(II)/tetraglycine complex by oxygen in the presence of luminol: mechanistic considerations. Anal. Chim. Acta 517 (2004): 125-130.
- [43] Araujo, C. S. T.; de Carvalho, J. L.; Mota, D. R.; de Araujo, C. L.; and Coelho, N. M. M. Determination of sulphite and acetic acid in foods by gas permeation flow injection analysis. Food Chem. 92 (2005): 765-770.
- [44] Carballo, R.; Dall'Orto, V. C.; Lo Balbo, A.; and Rezzano, I. Determination of sulfite by flow injection analysis using a poly[Ni-(protoporphyrin IX)] chemically modified electrode. Sens. Actuators, B 88 (2003): 155-161.
- [45] Kass, M.; and Ivaska, A. Spectrophotometric determination of sulphur dioxide and hydrogen sulphide in gas phase by sequential injection analysis technique. Anal. Chim. Acta 449 (2001): 189-197.
- [46] Azevedo, C. M. N.; Araki, K.; Toma, H. E.; and Angnes, L. Determination of sulfur dioxide in wines by gas-diffusion flow injection analysis utilizing modified electrodes with electrostatically assembled films of tetra-ruthenated porphyrin. Anal. Chim. Acta 387 (1999): 175-180.
- [47] Iland, P.; Ewart, A.; and Sitters, J. Techniques for Chemical Analysis and Stability Tests of Grape Juice and Wine. South Australia: Patrick Iland Wine Promotions, 1993.
- [48] Lu, J.; Dreisinger, D. B.; and Cooper, W. C. Anodic oxidation of sulphite ions on graphite anodes in alkaline solution. J. Appl. Electrochem. 29 (1999): 1161-1170.

- [49] Glasstone, S.; and Hickling, A. Studies in electrolytic oxidation. Part III. The formation of dithionate by the electrolytic oxidation of potassium sulphite. J. Chem. Soc. (1933): 829-836.
- [50] Sullivan, J.J.; Hollingworth, T.A.; Wekell, M.M.; Meo, V.A.; Etemad-Moghadam, A.; Phillips, J.G.; and Gump, B.H. Determination of free (pH 2.2) sulfite in wines by flow injection analysis: collaborative study. J. Assoc. Off. Anal. Chem. 73 (1990): 223-226.
- [51] Official Method 990.30 Official Methods of Analysis of AOAC International. Maryland: AOAC International, 2000.
- [52] Official Method 990.29 Official Methods of Analysis of AOAC International. Maryland: AOAC International, 2000.



สถาบันวิทยบริการ
จุฬาลงกรณ์มหาวิทยาลัย



APPENDICES

สถาบันวิทยบริการ
จุฬาลงกรณ์มหาวิทยาลัย

APPENDIX A

Results for the determination of free and total SO₂ in wines by SIA method

Table A1 Linear equations of calibration curve for the calculation of free and total SO₂ and dilution factor for the calculation of total SO₂

Wine sample	Linear equation ^a of calibration curve for free and total SO ₂ calculation	Dilution Factor for total SO ₂ calculation
White wine 1	$y = 11.518x + 8.314$ ($R^2 = 0.9992$)	5
White wine 2	$y = 11.252x + 13.220$ ($R^2 = 0.9985$)	5
Red wine 1	$y = 8.928x + 13.340$ ($R^2 = 0.9993$)	5
Red wine 2	$y = 6.973x + 2.837$ ($R^2 = 0.9996$)	5

^a y is signal current and x is concentration of SO₂

สถาบันวิทยบริการ
จุฬาลงกรณ์มหาวิทยาลัย

Table A2 Signal currents obtained by SIA method and concentration of free and total SO₂ in wine

Wine sample	Free SO ₂		Total SO ₂	
	Current ^a (nA)	Concentration of SO ₂ in wine (mg L ⁻¹)	Current ^a (nA)	Concentration of SO ₂ in wine (mg L ⁻¹)
White wine 1	139.9	11.4	122.9	49.7
	138.8	11.3	118.6	47.9
	133.2	10.8	120.3	48.6
	Average	11.2	Average	48.7
White wine 2	281.4	23.8	242.2	101.8
	287.8	24.4	242.5	101.9
	283.5	24.0	246.5	103.7
	Average	24.1	Average	102.4
Red wine 1	118.3	11.8	111.2	54.8
	118.5	11.8	110.8	54.6
	121.8	12.1	113.5	56.1
	Average	11.9	Average	55.2
Red wine 2	38.5	5.1	48.6	32.8
	38.0	5.0	46.4	31.1
	39.1	5.2	50.1	33.9
	Average	5.1	Average	32.6

^a Average current from four consecutive injections of wine sample

APPENDIX B

Results for the determination of free and total SO₂ in wines by titration method

Table B1 Concentration of standard I₂ and volume of blank for the calculation of free and total SO₂ in wines

Wine sample	Concentration of standard I ₂ (M)	Volume of blank ^a (mL)	
		Free SO ₂	Total SO ₂
White wine 1	0.01012	0.15	0.10
White wine 2	0.01012	0.30	0.15
Red wine 1	0.00993	0.20	0.15
Red wine 2	0.00993	0.35	0.20

^a The amount of iodine consumed by other matrix compounds in wine

Table B2 Volume of I₂ obtained by titration method and concentration of free and total SO₂ in wine

Wine sample	Free SO ₂		Total SO ₂	
	Volume of I ₂ ^a (mL)	Concentration of SO ₂ in wine (mg L ⁻¹)	Volume of I ₂ ^a (mL)	Concentration of SO ₂ in wine (mg L ⁻¹)
White wine 1	1.05	11.7	1.50	45.4
	1.05	11.7	1.60	48.6
	1.10	12.3	1.60	48.6
	Average	11.9	Average	47.5
White wine 2	2.00	22.0	3.40	105.3
	2.05	22.7	3.45	106.9
	2.00	22.0	3.40	105.3
	Average	22.2	Average	105.8
Red wine 1	1.15	12.1	2.00	58.8
	1.10	11.4	1.95	57.2
	1.10	11.4	2.00	58.8
	Average	11.7	Average	58.3
Red wine 2	0.75	5.1	1.15	30.2
	0.80	5.7	1.20	31.8
	0.75	5.1	1.25	33.4
	Average	5.3	Average	31.8

^a The amount of iodine consumed by SO₂ and other matrix compounds in wine

VITA

Mr. Chakorn Chinvongamorn was born on August 16, 1970 in Ratchaburi, Thailand. In 1989, he received the scholarship from the Thai government under the Development and Promotion of Science and Technology Talents Project (DPST) for the bachelor and master course. He received his Bachelor's degree of Science (Chemistry) from Kasetsart University in 1993 and Master's degree of Science (Chemistry) from Chiang Mai University in 1996. Then he worked at the Faculty of Science and Technology, Rajamangala University of Technology Thanyaburi until 2003.

Since 2003, he has become a graduate student at the Department of Chemistry, Faculty of Science, Chulalongkorn University and worked under the supervision of Associate Professor Orawon Chailapakul. In 2004, he has received the scholarship from the Thailand Research Fund through the Royal Golden Jubilee Ph.D. Program. He had an opportunity to do the research in Prof. Toshihiko Imato's group at Kyushu University for ten months in 2005. He graduated the Doctor of Science degree from Chulalongkorn University in the academic year 2007.

Publication

- [1] Chinvongamorn, C.; Pinwattana, K.; Praphairaksit, N.; Imato, T.; and Chailapakul, O. Amperometric Determination of Sulfite by Gas Diffusion-Sequential Injection with Boron-Doped Diamond Electrode. *Sensors* 8 (2008): 1846-1857.

สถาบันวิทยบริการ
จุฬาลงกรณ์มหาวิทยาลัย